



ISSN 2314-5609  
Nuclear Sciences Scientific Journal  
7, 1- 30  
2018  
[http:// www.ssnma.com](http://www.ssnma.com)

## LATE PRECAMBRIAN ACIDIC VOLCANICS SOUTH SINAI, EGYPT: IMPLICATIONS FOR GEOLOGY AND RADIOACTIVITY

MOHAMED S. AZAB  
*Nuclear Materials Authority, Egypt*

### ABSTRACT

Three extrusions of Late Precambrian acidic volcanic, south Sinai, Egypt are selected for studying their geology and radioactivity. Field observations revealed that, these volcanic rocks are believed to have erupted later than the Dokhan volcanics. These volcanic rocks are represented mainly by lava flows of rhyolitic composition, lithic and crystal tuffs. They have many geochemical characteristics of metaluminous to peraluminous A-type magma that were emplaced into within plate tectonic environment and evolved through differentiation processes from mantle-derived basaltic magma with noticeable crustal contribution. The fractionation of plagioclase in the early formed basaltic rocks leads to the pronounced negative Eu anomaly displaced by these volcanics. These volcanics are considered as source for uranium since they contain more than 8 ppm average uranium content. The average thorium and uranium contents are 17ppm and 15 ppm for Ras Naqab volcanics, 16.7 ppm and 8.5 ppm for Iqna Sharaya while Umm Shouki volcanics have 17 ppm average Th and 8.6 ppm average U. Three modes of uranium occurrence are inferred. The first assumes incorporation of U and Th within accessory minerals such as zircon, monazite and uranotorite where thorium is three times more abundant than uranium. In the second case, uranium is equal to one half of the thorium or slightly more which indicates that a process of uranium enrichment (U-gain) may be occurred. In this case, uranium is adsorbed on ferroxides, altered minerals, or along grain boundaries. When uranium is less than one quarter of thorium or completely disappear, a process of uranium leaching (U-loss) may take place.

The U & Th-bearing rare earth mineral tornebohmite is classified as tornebohmite-Ce where its Ce content is about 39.40 wt %. Tornebohmite may be formed by hydrothermal fluids penetrating the studied volcanics. These fluids may be accompanied and contemporaneous with the syenogranite intrusion which occurs at the southwestern part of Ras Naqab area.

### INTRODUCTION

In the Eastern Desert and Sinai, Egypt, there are three prevailed episodes of volcanic activity. The first two of them are essentially calc-alkaline, while the third one has alkaline to peralkaline affinity. The first episode is the oldest and has 800–700 Ma old, (Harris et al., 1984; Kroner, 1985 and Stern et al., 1991). It produced the island arc Younger Metavolcanics which are associated with volcanoclastics and

metamorphosed within the greenschist facies (Stern, 1981). The second episode of volcanic activity was dated 620–580 Ma old (Stern, 1981; Bielski, 1982, Bentor, 1985 ; Ressetar and Monrad, 1983; Abdel-Rahman and Doig, 1987) and produced the Dokhan Volcanics. It is occasionally intercalated with molasse-type Hammamat clastic sediments (Gass, 1982; El-Gaby et al., 1988, 1989, 1990, 1991; Moussa, 2003) and erupted after the accretion of the

island arc onto the East Saharan Craton. The third episode, the youngest, produced the so called Katherina Volcanics and was originated after the closure of the Pan-African orogeny (Agron and Bentor, 1981). These alkaline eruptions form limited but widely scattered outcrops extended allover the Arabian–Nubian Shield (ANS), and together with the associated alkali granites mark the transition to intraplate alkaline magmas, which prevailed during the Phanerozoic (Bentor, 1985; Stern et al., 1988; Black and Liegeois, 1993).

At the southern part of Sinai, the three volcanic episodes are represented. The first one was recorded at Wadi Kid ( El-Gaby et al. 1991), Wadi Malhag (Ghoneim et. al.,1989) and Wadi Um Adawi (Ahmed ,1985). The second phase of volcanicity was outcropped at Wadi Kid ( El-Gaby et al. 1991). The third one was recorded at Katherine area (Eyal and Hezkiyahu, 1980; Bielski,1982; Bentor, 1985; El-Morsy,1988; El Masry ,1991; and El- Masry et al.,1992), Iqna Sharaya area (Eyal et. al., 1980; Bentor. 1985; Bentor and Eyal, 1987; Sherif, 1992; El Metwally,1997 and Samuel et al.,2001) and Um Shuoki area (Shimron,1980; Bentor and Eyal, 1987; Abu El. Leil et al., 1990; Khalaf et al., 1994; El Sayed, 1993 and El-Masry,1998).

Three extrusions of Late Precambrian acidic volcanic south Sinai, Egypt are selected for studying their geology and radioactivity. The first one is located at Wadi Iqna, south Sinai, the second is outcropping at Wadi Umm Shouki, southeastern Sinai whereas the third one is exposed at Ras El-Naqab plateau, eastern Sinai.

The previous radioactivity studies carried out on the acidic volcanic rocks of south Sinai are quiet restricted (Sherif, 1992, El Sayed, 1993, Azab, 2002 and Sherif et al.,2007). So, it is intended to examine these volcanics with respect to their radioactivity. In order to achieve this goal, attention was focused to these volcanics to elucidate their field situation. Their petrography was thoroughly examined to determine their mineral composi-

tion and the significance of their textures. The petrogenesis of these volcanics was discussed through studying their geochemistry. Their radioactivity is also considered to indicate the distribution of uranium and thorium as well as the radioactive minerals.

Zircon, monazite, uranothorite and tornebohmitite minerals are analysed and identified by ESEM.

## GEOLOGIC OUTLINE

The selected three areas for the present study are located at south Sinai Governorate (Fig. 1). The figure is also showing the geology of these localities which will be discussed on the following paragraphs.

### Ras El-Naqab Volcanics

The Ras El-Naqab volcanics cover about 80 km<sup>2</sup> and located immediately at the border line separating between Sinai, Egypt and Palestine. These volcanics were described by Agron and Bentor, (1981) and Mushkin et al. (1999) as Biq'at Hayareah and Neshef Massif respectively while it was named as Gabal Hamra in the geologic map of Egypt (EGSMA 1981). These volcanics occur as small hilly cones with steep slopes (Fig.2) attaining 950m above the sea and composed mainly of tuffs, lava flows, porphyritic rhyolites and pyroclastics. Extrusive rhyolites are the most abundant without mutual contacts with their volcanic counterparts. They are fine to medium grained with brown colour having abundant quartz and potash feldspar phenocrysts. The pyroclastics are less abundant and composed mainly of lapilli and ash tuffs. Ras El-Naqab volcanics form continuous ridge dipping to E and ENE (direction of African Rift Valley). These dips result from a regional tilt which occurred in Neogene times in connection with the formation of the rift valley. During this period, the Precambrian rocks of Ras El-Naqab volcanics were first exposed (Agron and Bentor, 1981). This uplifting process led to throwing down the Phanerozoic sedi-

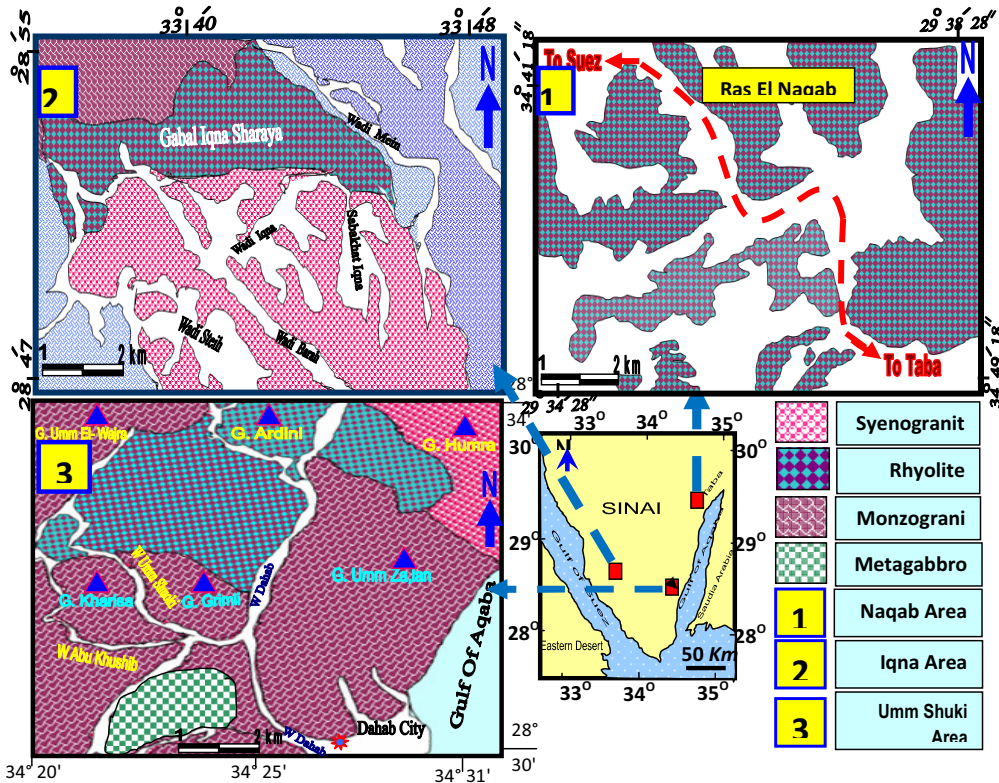


Fig. 1: Locations and geologic maps for the studies areas, southern and eastern Sinai, Egypt.  
 1- Ras Naqab acidic volcanics, Eastern Sinai; 2- Iqna volcanics, south Sinai.  
 3- Um Shuki acidic volcanics, southeastern Sinai



Fig. 2: Widely scattered volcanic hilly cones of Ras El-Naqab area

ments toward the west producing normal fault (Fig.3). To the western extremity of the area, these volcanics are found to be unconformably overlain by Cambrian sandstones (Fig. 4) which suggest their Precambrian age. At Wadi Khileifyia, these volcanics are extruding the monzogranite (Fig. 4) and intruded by syenogranite (Azab, 2002). These volcanics are related to the Feirani group volcanic rocks of Abu El-Leil et al. (1990) and Wadi Ager volcanics (Iqna volcanics) of Eissa (2000).

### The Iqna Sharay'a Volcanics

The Iqna Sharay'a volcanics are generally very hard, massive, with greyish brown colour

and spotted with pinkish and white phenocrysts of potash feldspar, plagioclase and quartz. The phenocrysts are fine to medium-grained while others have coarse-grained ones. They consist mainly of rhyolite and porphyritic rhyodacite with subordinate sheets of ignemberites.

The contacts between these rock varieties are gradational. This reveals a series of flows within these volcanics. The examined volcanics form an elongated curved mass trending roughly from west (the west extension of the map) to east and cover about 26 km<sup>2</sup> (Fig. 1). The present volcanics intruded by the syenogranite with an intrusive sharp contact (Fig.5)

and intruding the monzogranite at Wadi Baraq (Fig.6). The volcanic rocks of Iqna Sharay'a area are equivalent to the so called Farsh zubeir quartz syenites and volcanics described by El Gammal (1986) and Sherif (1992) at Wadi El Akhdar to the south of Iqna Sharay'a area where these rocks are intruded by the syenogranites and intruding the monzogranite of Gabal Main.

#### Um Shuki Volcanics

The exposed volcanic rocks of Um Shuoki area (about 30Km<sup>2</sup>, Fig. 1) are belonging to the Feirani Group (Shimron, 1980) or Dahab for-

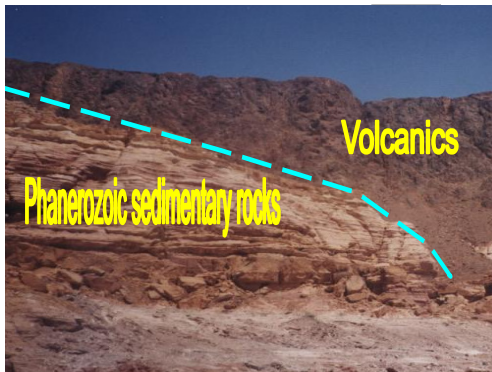


Fig. 3: Normal fault showing the throwing down of Paleozoic sediments, Ras El-Naqab area.



Fig. 5: Sharp contact between the volcanics and the syenogranite of Iqna Sharay'a area

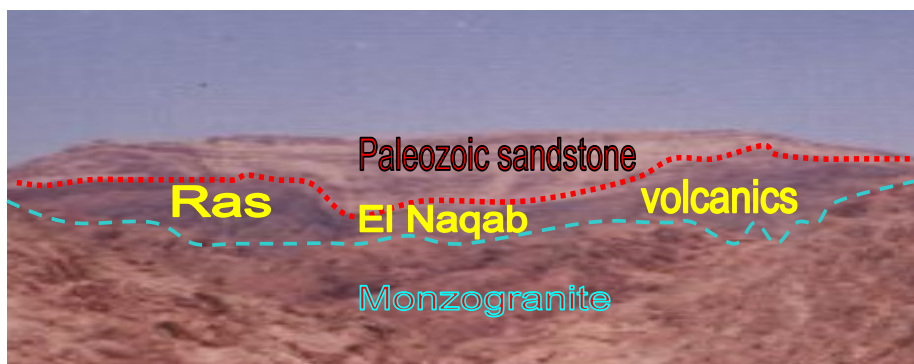


Fig. 4: Ras El-Naqab volcanics unconformably overlain by Paleozoic sandstone



Fig. 6 : Sharp contact between the volcanics and the monzogranite of Wadi Baraq ,Iqna Sharay'a area



Fig. 7: Sharp contact between the volcanics and the syenogranite of Umm Shuoki area

mation and Nasab formation of Feirani Group (Abu El-Leil et al., 1990 and El-Masry, 1998). The studied volcanic rocks form lava flows, sills and small subvolcanic intrusions. They consist mostly of rhyolites and subordinate rhyodacite with minor pyroclastics that occur as interlayers with the rhyolites and rhyodacite. These volcanics are mostly composed of quartz, potash feldspar and subordinate plagioclase phenocrysts in very fine grained groundmass. The pyroclastics are generally containing rock fragments of monzogranite, older granites and some basic volcanics to suggest the older age of these rock fragments.

In conclusions, the examinations of the field relationships of the studied volcanics reveal that:

These volcanics are intruded by the syenogranite (Phase III younger granites) (Fig.7) where some apophyses and offshoots of the Phase III younger granites extending into the volcanics. It also noticed that these volcanics are invading directly through the monzogranite (Phase II younger granites) (Fig.8). So, these volcanic rocks are believed to have erupted later than the Dokhan volcanics (Abu El-Leil et al., 1990 and Azab, 2002). The setting of these volcanics that confined between the two phases of the younger granite is confirmed by the studying of Bendor, 1985

; Stern and Hedge, 1985; Bendor and Eyal, 1987; Kröner et al., 1990; Stern, 1994; Garfunkel, 1999; Moghazi, 1998–2002; Jarrar et al., 2003; Katzir et al., 2007b; and Jarrar et al., 2008. They stated that the evolution of the Arabian–Nubian Shield was passed through four stages of magmatic activity, the latest one is characterized by within-plate alkaline and peralkaline granite suite preceded by intensive bimodal volcanism formed at ~600–550 Ma.

-The pyroclastics are generally contain rock fragments from each of the older granites and the monzogranite (phases II of the younger granites) which suggest that these volcanics



Fig. 8: Sharp contact between the volcanics and the monzogranite of Umm Shuoki area

are postdating the precursors of these rock fragments.

-The volcanic rocks are always intruded by the syenogranite (phase III of the younger granites) indicating that these volcanics are often predating these granites.

- Consequently, the studied volcanics have a field situation that included between the two phases of the studied granites. So, these volcanic rocks are believed to have erupted later than the Dokhan volcanics.

-The contacts between the studied volcanic phases are generally gradational to suggest their derivation from the same magma source.

### PETROGRAPHIC INVESTIGATIONS

Microscopically, the studied volcanics can be distinguished into lavas and tuffs. The lavas are mainly represented by porphyritic rhyolites and the associated rhyolites (Ras El-Naqab volcanics), while Igna Sharayi and Um Shuki volcanic contain rhyodacite together with porphyritic rhyolites and rhyolites.

The tuffs are outcropping at Ras El-Naqab and Um Shuki areas and represented by vitric, crystal and lithic tuffs. The following is the petrographic description of lavas, while tuffs will be described later.

#### Lava Flows

Lava flows are ranging in their composition from dacite to rhyolite. They usually have aphanitic phyric textures. The main constituents of phenocrysts are quartz, sanidine, and plagioclase feldspars which embedded in a microcrystalline felsic groundmass. The groundmass is composed essentially of quartz, potash feldspars, plagioclase feldspar, and riebeckite in addition to few zircon, apatite, and iron oxides as accessory minerals. (Fig.9). *Quartz* presents as euhedral to subhedral crystals and as anhedral aggregates. They usually serrated and reveal andulous extinction and embayment structure with groundmass. The

quartz phenocrysts are partially corroded and replaced by the groundmass (Fig.10).

#### Potash feldspars

Potash feldspars occur as subhedral to anhedral crystals and represented mainly by orthoclase microperthite and occasionally by sanidine. *Orthoclase* microperthite exhibits microperthetic texture. Some phenocrysts of potash feldspar enclose small quartz crystals and some patches from the surrounding

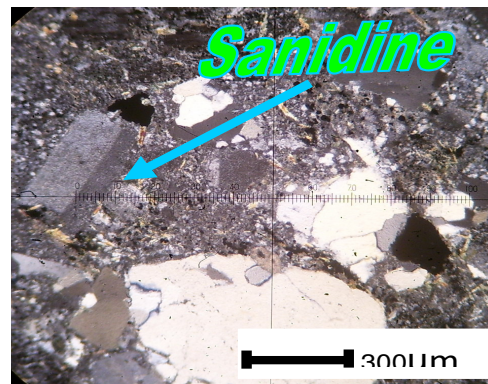


Fig.9: Photomicrograph showing sanidine and quartz phenocrysts embedded in a microcrystalline felsic groundmass, XPL

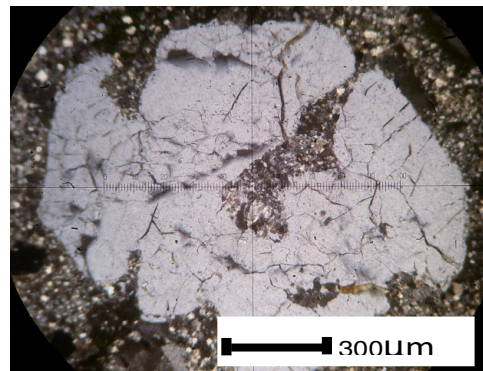


Fig.10: Photomicrograph showing quartz phenocryst partially replaced by the groundmass, crossed polars, XPL

groundmass (Fig.11) and generally display simple twinning. *Plagioclase* feldspar occurs as small subhedral to anhedral laths that partly altered to sericite and corroded by the surrounding groundmass. It displays lamellar twinning. The deformational effects are displayed by the presence of undulose extinction and deformed lamella of quartz and plagioclase respectively.

### Riebeckite

Riebeckite rarely occurs either as small corroded platy shaped crystals or as spongy aggregates. They are moderately altered and most of them are chloritized and replaced by small flak of biotite (Fig.12). The presence of riebeckite in the porphyritic rhyolite reflects the alkaline nature of the magma from which it was originated. Also, the presence of biotite together with riebeckite suggests the hydrous nature of this magma.

The groundmass has felsitic texture and comprising aggregates of quartz, potash feldspars, plagioclase, riebeckite in addition to few zircon, apatite, and iron oxides.

The studied lava flow is generally showing spherulitic texture ( Fig.13) which is composed of radial fibers of potash feldspar and quartz. Spherulites are formed in response to

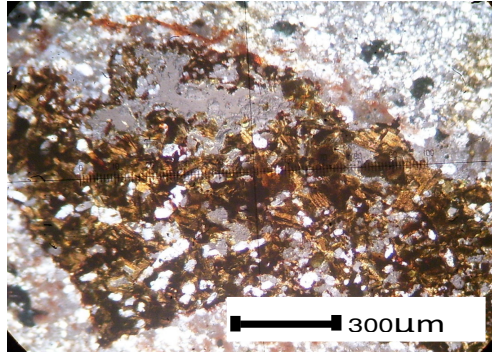


Fig. 12: Photomicrograph showing altered riebeckite to biotite, XPL

the drastic under cooling of viscous silicate melts (Lofgren, 1974).

### The Tuffs

Microscopically, tuffs are classified according to their essential constituents into vitric tuffs, crystal tuff and lithic tuffs. On the following paragraphs, a brief description for every rock unit will be given.

### Vitric tuffs

Vitric tuffs are generally classified into crystal vitric tuffs as well as lithic vitric tuffs

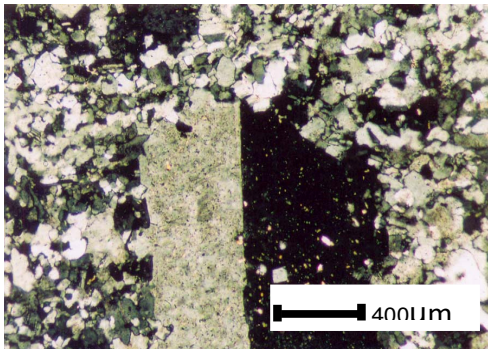


Fig. 11: Photomicrograph showing potash feldspar phenocryst enclosing small quartz crystals, crossed polars, XPL

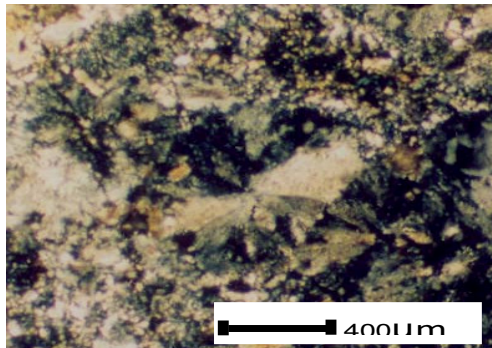


Fig. 13: Photomicrograph shows spherulitic texture in porphyritic rhyolite, XPL

which can be described independently as follows.

#### *Crystal vitric tuffs*

They are composed of quartz, potash feldspar and plagioclase fragments set in a fine (ash) tuffaceous groundmass (Fig.14).

Quartz occurs as anhedral monocrystalline grains similar to the so-called volcanic quartz. It corrodes the potash feldspar crystal and partially embayed by the groundmass to suggest solid state growth (Fig.14). Alkali feldspar occurs as subhedral orthoclase microperthite with cloudy turbid brown appearance due to extensive alteration (Fig.14). It shows partial embayment by the groundmass and banded twisted habit due to deformation effects (Fig.14). *Plagioclase* feldspar displays turbid appearance and lamellar twinning with partial alteration to sericite (Fig.14).

#### *Lithic vitric tuffs*

They are composed mainly of granitic rock fragments with main constituents of quartz and feldspars (Fig.14). They have irregular and sinuous boundaries due to their replacement by the hot groundmass materials. The grain-boundary textures of the quartz crystals, within the granitic rock fragment, such as ser-

rated, sutured and polygonal textures together with wavy extinction (Fig.14) indicate that they were underwent thermal and deformational effects.

#### **Crystal tuffs**

Crystal tuffs has an aphanitic fragmental texture and are characterized by the presence of high percentage of quartz and feldspars crystal fragments that ranging in size between medium- and very fine-grained. Quartz occurs as strongly deformed microcrystalline anhedral grains embayed by the groundmass materials (Fig.15). Solid state growth is indicated by groundmass embayment and inclusion within quartz grains.

Some quartz phenocrysts are embayments with sharp corners. Donaldson and Henderson (1988) stated that embayment can result from unstable primary growth. If an embayed crystal has sharp corners and edges, and if the included zones of the groundmass follow the shape of the embayments, then primary disequilibrium growth rather than corrosion is the cause. The crystal fragments of feldspars are mostly composed of strained tabular grains of plagioclase as well as subordinate potash feldspar microperthite. The plagioclase grains

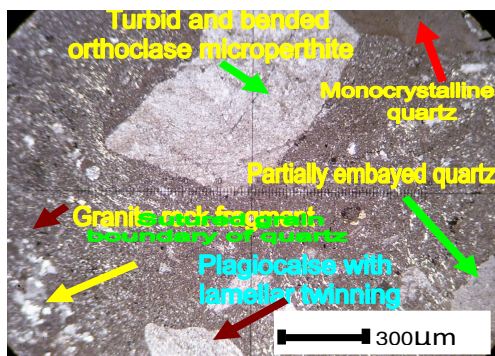


Fig. 14: Photomicrograph shows crystal vitric tuffs and lithic vitric tuffs, XPL

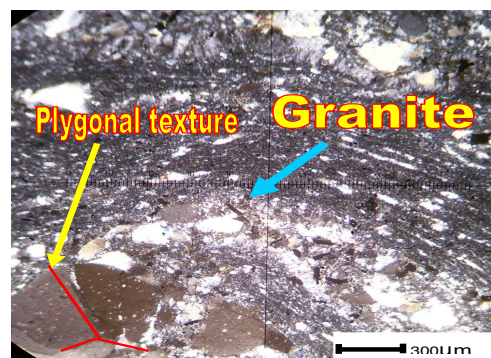


Fig. 15: Photomicrograph showing partially assimilated granite rock fragments set in eutaxitic groundmass as well as polygonal texture of quartz, XPL

are markedly distinguished by murky-brown alteration surfaces and dislocated twin lamellae due to deformational effects.

### Lithic tuffs

The principal components of the lithic tuffs consist of lithic fragments of granite set in rhyolitic groundmass. These granitic rock fragments are composed mainly of quartz, potash and plagioclase feldspars. The grain boundary textures of quartz such as polygonal and serrated and sutured boundaries (Fig.15) indicate their recrystallization due to thermal effects of the hot groundmass. The granite rock fragment (Fig.15) is folded, distorted and followed the same direction as that produced by the groundmass. This feature indicates that the granite rock fragment was semi-molten during the formation of the groundmass. It is noticed that the granitic fragments are partially assimilated by the hot groundmass as indicated by its diffused contact and by its invasion by the hot components of this groundmass (Fig.15). The microcrystalline groundmass shows well developed eutaxitic texture (Fig. 15).

## PETROCHEMISTRY

### Analytical Techniques

Fifteen representative fresh samples were chosen, from the studied volcanics in the selected three areas, for major, trace and rare-earth elements analyses. The major constituents were determined following the method of Shapiro and Brannock (1962) modified by El-Reedy (1984).  $\text{SiO}_2$ ,  $\text{Al}_2\text{O}_3$ ,  $\text{TiO}_2$  and  $\text{P}_2\text{O}_5$  were determined by colourimetric spectrophotometry.  $\text{CaO}$ ,  $\text{MgO}$ ,  $\text{Fe}_2\text{O}_3$  and both  $\text{Na}_2\text{O}$  and  $\text{K}_2\text{O}$  by flame photometer while  $\text{MnO}$  was determined by atomic absorption. The trace elements were determined by XRF technique. The XRF analyses were carried out on a Phillips Sequential X-ray spectrometer system X'Unique. The program used for the calculation was X-40. Error factor in the machine

is  $\pm 2$  rel %. The analyses were carried out in the Nuclear Materials Authority of Egypt. The rare-earth elements concentrations were determined by neutron activation analysis with at least two standard reference materials at the Technical University of Budapest, Hungary. The results of these analyses are tabulated and given in Table (1).

### Chemical Composition

The detailed chemical data of 15 representative samples from the three selected localities, five samples per each area, are represented in Table (1).

Based on the geochemical data given in Table (1), a number of correlation and discrimination diagrams are used in order to identify the nomenclature, magma type, tectonic setting and the petrogenesis of the studied volcanics.

Figure (16) was constructed which shows that the differences between the three averages of the studied volcanics are rather limited and restricted to the variation in the content of Al, Na and K. The volcanics of El Naqab area have lower Al content relative to the other two areas which may ascribe to the alteration of k-feldspar. Iqna Sharaya volcanics have high Na content due to their content of alkali amphibole present while the volcanics of El Naqab and Umm Shouki areas have nearly the same Na content. The K-contents of Ras Naqab volcanics are remarkably varied and is the highest among the volcanics of the three areas because of the varied degrees of K- metasomatism prevailing after the emplacement of these volcanics. This can be easily noticed in El Naqab volcanics. Furthermore, the rhyolite of the Eastern Desert of Egypt which was studied by El-Gaby et al. (1989), Table 2 has a relatively identical average values for all oxides except for Na and K compared with averages of the studied volcanics. The sodium content in Iqna Sharaya is higher in comparison with those of the other areas while its potassium content is low relative to the other areas. The

Table 1 : Major, trace and rare-earth elements analysis of the studied volcanics

	NQ1	NQ2	NQ3	NQ4	NQ5	US1	US2	US3	US4	US5	IQ1	IQ 2	IQ 3	IQ 4	IQ 5
<b>Major Oxides</b>															
SiO <sub>2</sub>	76.0	74.9	72.9	78.7	73.8	75.6	76.7	71.9	73.0	76.4	72.5	72.10	72.30	72.62	73.39
TiO <sub>2</sub>	0.19	0.24	0.26	0.19	0.23	0.23	0.30	0.34	0.25	0.22	0.52	0.32	0.41	0.37	0.31
Al <sub>2</sub> O <sub>3</sub>	11.5	11.6	11.9	12.8	11.9	13.7	13.3	13.8	13.7	13.6	12.9	13.79	13.77	13.36	13.77
Fe <sub>2</sub> O <sub>3</sub>	2.34	2.25	2.95	2.40	2.40	3.59	1.80	3.83	2.82	1.01	1.9	2.04	2.16	2.49	1.76
FeO	0.80	0.70	1.30	0.74	0.70	1.40	0.13	1.97	0.58	0.21	0.2	0.8	0.82	0.54	0.29
MnO	0.03	0.16	0.04	0.03	0.15	1.03	0.31	1.4	0.20	0.17	0.03	0.08	0.07	0.07	0.08
MgO	0.17	0.21	0.36	0.26	0.27	0.27	0.27	0.51	0.35	0.30	2.4	1.0	0.99	1.00	0.8
CaO	0.82	0.77	0.38	0.37	0.46	0.30	1.77	1.22	1.17	0.44	1.68	1.80	1.84	1.8	1.47
Na <sub>2</sub> O	3.33	0.30	1.19	3.37	2.37	0.13	0.34	0.47	1.92	4.70	4.5	4.24	4.21	4.64	4.37
K <sub>2</sub> O	4.5	8.60	8.17	4.45	7.50	4.17	5.01	4.49	5.7	2.87	3.2	3.67	3.30	2.91	3.10
P <sub>2</sub> O <sub>5</sub>	0.02	0.01	0.02	0.01	0.01	0.02	0.04	0.04	0.10	0.03	0.1	0.09	0.11	0.10	0.12
Total	99.7	99.74	99.87	99.95	99.79	99.94	99.97	99.97	99.79	99.95	99.93	99.93	99.98	99.9	99.98
<b>Trace Elements</b>															
Ba	82	306	325	28	118	173	400	508	370	287	50	406	512	314	427
Cr	2	4	5	1	3	1	2	4	1	1	106	112	131	103	77
Nb	54	40	39	60	44	18.1	10.6	15	13	15	4	197	289	109	213
Ni	3	6	6	2	5	3	7	1	3	6	15	18	16	18	18
Rb	176	210	170	177	160	145	180	191	196	106	50	35	17	120	16
Sr	18	17	15	14	17	40	155	96	174	98	63	190	116	267	111
Y	103	55	106	66	65	43	27	30	31	32	21	65	39	92	37
Zn	105	26	56	123	29	82	70	99	79	79	9	9	21	15	11
Zr	825	444	550	956	560	334	226	340	350	420	520	450	720	810	525
V	8	6	5	5	5	5	1	4	7	3	3	5	5	16	4
Co	3	2	3	1	2	3	5	2	4	1	3	17	29	160	19
Cu	25	22	12	33	11	4	0	5	6	8	24	20	21	22	23
Ga	29	26	24	30	27	22	19	20	23	19	98	58	41	99	62
Pb	24	15	46	35	20	8	65	18	63	23	53	49	44	28	53
<b>Rare-earth elements</b>															
La	86	45	50	94	66	34	35	70	29	38	55	48	87	65	75
Ce	177	108	99	224	160	99	80	127	60	75	150	100	102	220	150
Pr	21	12.8	12.5	25.5	12	11	8	14	8	9	18	12	13	18	14
Nd	84	54	53	110	73	32	55	32	34	33	80	50	55	99	78
Sm	18	12	11	22	10	13	7	10	8	10	17	12	13	21	14
Eu	0.8	0.9	1.5	0.7	1.2	1.5	2.1	2.03	0.67	0.8	0.8	0.7	0.9	0.6	1.2
Tb	3	2	2	3	1	1.9	0.89	1.05	1.8	1.98	2	3	1	1.5	1.9
Dy	16.5	10	12	18	15	5.7	5.19	6.09	6.77	5.99	13	15	11	10	16
Ho	3.2	2	2.5	3.5	3.3	1.09	1.28	1.99	1.87	1.68	2.2	3.2	3.1	2	2.5
Er	9.8	6	8	10	7	3.08	3.43	3.77	3.34	4.08	8.5	7	6	8	7.5
Tm	1.5	0.8	1.1	1.5	1.3	0.54	0.44	0.46	0.51	0.45	0.82	0.90	1.2	1.4	0.88
Yb	9	5.3	7	9.8	5	2.76	2.65	2.77	2.66	3.15	7	5	8	6	5.5
Lu	1.2	0.9	1	1.5	1.3	0.44	0.46	0.43	0.40	0.49	1.2	0.99	1.3	1.4	1.00
Ta	5	3	3	2	4	0.99	0.96	0.82	0.68	0.78	4	3	3.5	2	5

NQ = Ras El-Naqab volcanic ; US = Umm Shouki volcanic ; IQ = Iqna Sharaya volcanics

Table 2: The average chemical compositions of the studied volcanic and the rhyolite of the E.D. of El Gaby 1989

	SiO <sub>2</sub>	TiO <sub>2</sub>	Al <sub>2</sub> O <sub>3</sub>	Fe <sub>2</sub> O <sub>3</sub>	FeO	MnO	MgO	CaO	Na <sub>2</sub> O	K <sub>2</sub> O	P <sub>2</sub> O <sub>5</sub>
El-Naqab volcanics	75.26	0.222	11.94	2.468	0.735	0.082	0.254	0.56	2.0475	6.644	0.014
Umm Shouki volcanics	74.72	0.268	13.62	2.61	0.858	0.622	0.34	0.98	1.512	4.448	0.046
Iqna Sharaya volcanics	72.582	0.386	13.518	2.07	0.53	0.066	1.238	1.718	4.392	3.236	0.104
Av.Rhyo. E.D. El Gaby 1989	73.81	0.26	12.4	1.24	1.58	0.06	0.2	0.75	1.07	4.65	0.04

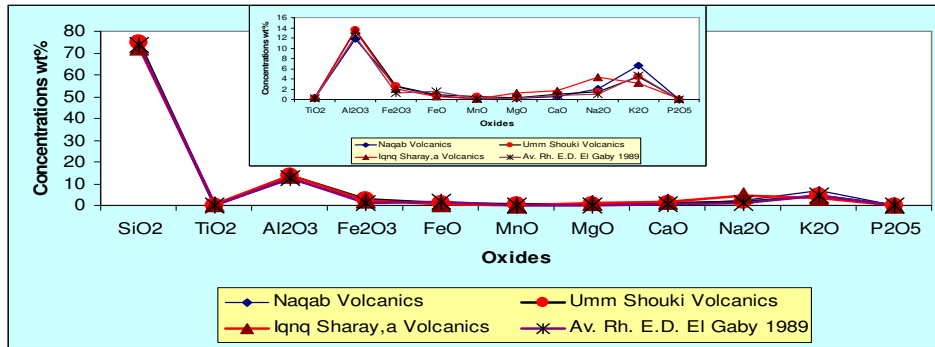


Fig. 16: The average chemical composition of the studied volcanics compared with the averages of the Eastern Desert of El Gaby (1989)

K-content in El Naqab volcanics is higher than those of the studied volcanics which may be due to K -metasomatism prevailing after the emplacement of these volcanics.

**PETROCHEMICAL NOMENCLATURE**

In order to nominate the studied volcanics using their chemical composition, Winchester and Floyd (1977) diagram was chosen which is based on using major and trace elements and hence a more sufficient identification is expected. The diagram is based on plotting SiO<sub>2</sub> versus Zr/TiO<sub>2</sub> (Fig.17). Samples of the studied volcanics were found to plot in rhyolite and rhyodacite/dacite fields. To confirm the nomenclature of the studied volcanics, their obtained data are plotted on the diagram of Cox et al. (1979), (Fig.18), where all the data points fall within the rhyolite field.

**Variation Diagrams**

For a better understanding of the geochemical evolution of the studied volcanic rocks and elucidate , whether these rocks constitute a cogenetic suite or not, some variation diagrams were constructed using the major and trace element data on the volcanic rocks.

**Harker diagrams**

This type of variation diagrams is used

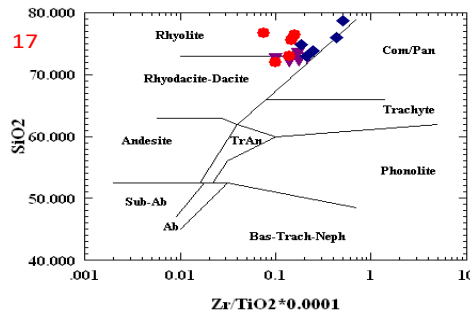


Fig. 17: Geochemical nomenclature of the studied volcanics (According to Winchester and Floyd,1977) : Naqab volcanics (blue diamonds), Iqna Sharay'a volcanics (red triangles) Umm Shouki volcanics (red circles)

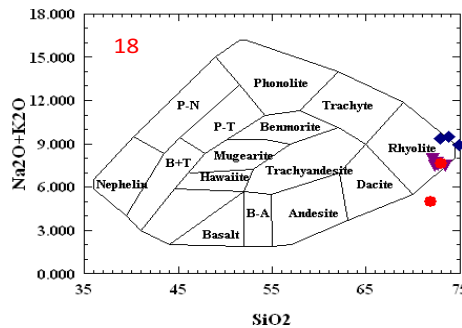


Fig.18: Geochemical nomenclature of the studied volcanic (According to Cox et al.,1979), symbols as on Fig.17

principally for illustrating the course of chemical evolution of magma liquids and for determining the differentiation trends in magmatic rocks. Figure (19) shows the plotting of weight percent of  $\text{SiO}_2$  versus some major oxides (wt %). The figure shows an overall negative correlation between  $\text{SiO}_2$  and each of  $\text{Al}_2\text{O}_3$ ,  $\text{CaO}$ ,  $\text{FeO}$ ,  $\text{TiO}_2$ ,  $\text{P}_2\text{O}_5$  and  $\text{MgO}$  whereas  $\text{Na}_2\text{O}$  exhibits positive correlation. The relationship between the plotting of  $\text{SiO}_2$  and  $\text{K}_2\text{O}$  is not clear and the noisy scatter of the data points is mainly attributed to the post magmatic alteration of the K-feldspar

presented in these volcanics. The figure also shows an overlap between the plotting of the data points of the studied volcanics and no compositional gaps exist which may indicate a cogenetic relationship between them and may suggest their derivation from the same magma source.

The plotting of selected trace elements (ppm) versus  $\text{SiO}_2$  wt% for all the studied volcanics (Fig. 20), is generally, showing that Co, Zn, Ni, V, Sr, Y, Ba, Cu and Cr have negative correlation with  $\text{SiO}_2$ . In details, in the course of magmatic differentiation Co, Cu,

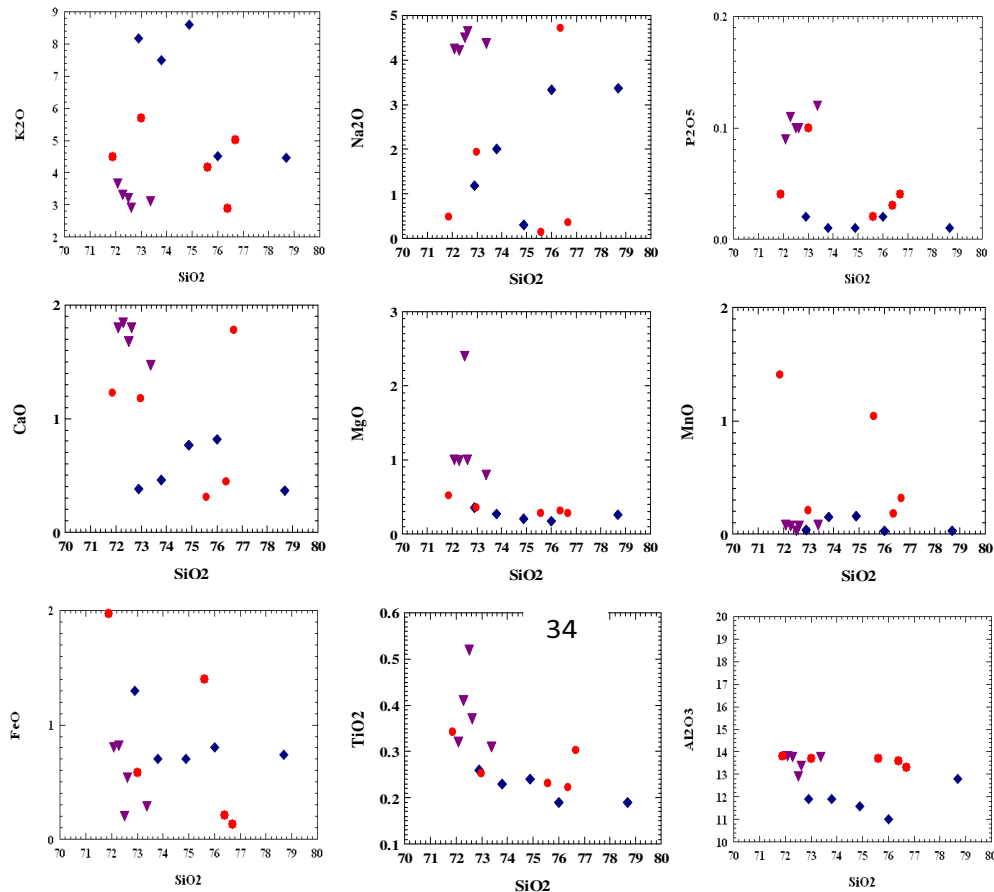


Fig. 19: :Harker variation diagrams of  $\text{SiO}_2$  plotted versus other oxides of the studied volcanics. Symbols are as on Fig. 17

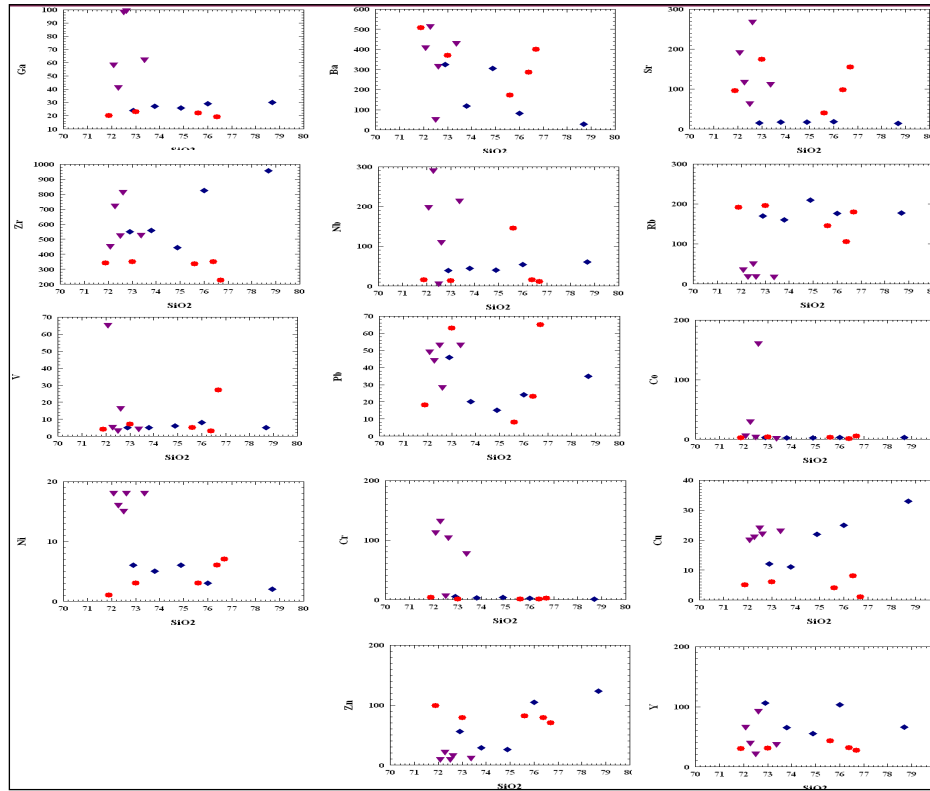


Fig. 20: Harker variation diagrams of  $\text{SiO}_2$  plotted versus selected trace elements (ppm) of the studied volcanics. Symbols are as on Fig. 17

Zn, Ni, V and Cr are in general considered to follow the iron and illustrate distinct large negative variation with  $\text{SiO}_2$ . This is logic behavior where these elements are fractionated from ferromagnesian minerals. The figure also shows that Zn, Pb, Rb, Zr and Ga have positive correlation where the contents of these elements are generally increased in the more differentiated rocks

#### Nature And Type Of Magma Of The Studied Volcanic Rocks

Some variation diagrams are used to elucidate the type of magma from which the volcanic rocks are originated. For example, the total alkali-silica diagram and the AFM diagram.

#### The total alkalis-silica diagram

This diagram was used by Irvine and Baragar(1971) to distinguish between alkaline and subalkaline rock suites. Figure (21) shows that all the studied volcanics fall within the subalkaline field. This field is further subdivided by Irvine and Baragar(1971) into tholeiitic and calc-alkaline fields as shown on the AFM diagram (Fig.22) where nearly all the data point of the studied volcanics are plotted within the calc-alkaline field .

The nature of the magma from which the studied volcanics are originated can be identified by plotting their data points on the diagram of Maniar and Peccoli (1989) (Fig 23). The figure shows that the samples are mostly

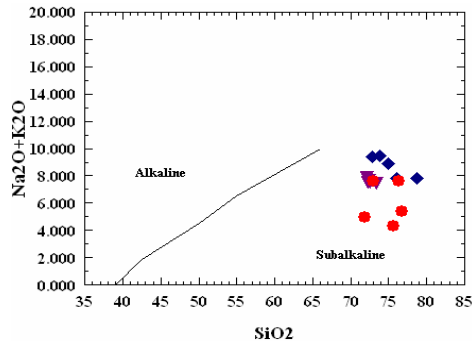


Fig. 21: Total alkalis versus  $\text{SiO}_2$  contents of the studied volcanics. The division of alkaline and subalkaline fields is after Irvine and Baragar(1971). Symbols are as on Fig. 17

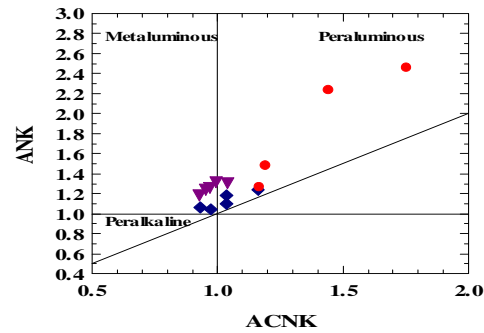


Fig. 23:  $\text{Al}_2\text{O}_3/\text{CaO} + \text{Na}_2\text{O} + \text{K}_2\text{O}$  binary diagram of the studied volcanics (According to Maniar and Peccoli,1989). Symbols are as on Fig. 17

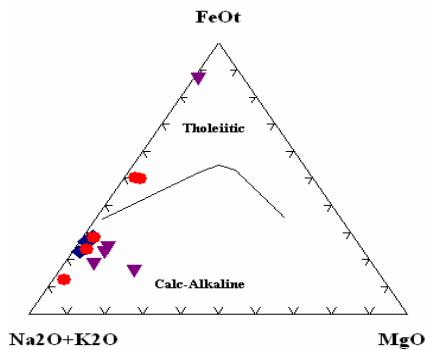


Fig. 22: Total alkalis- $\text{FeO}$ - $\text{MgO}$  diagram for the studied volcanics (According to Irvine and Baragar,1971). Symbols are as on Fig. 17

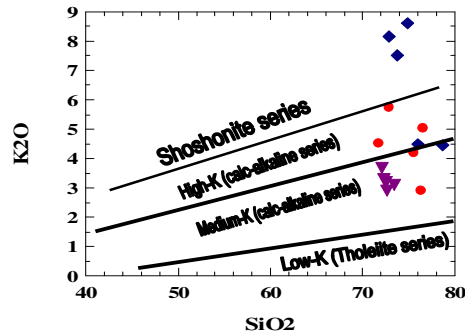


Fig. 24:  $\text{Al}_2\text{O}_3/\text{CaO} + \text{Na}_2\text{O} + \text{K}_2\text{O}$  binary diagram of the studied volcanics (According to Maniar and Peccoli,1989). Symbols are as on Fig. 17

plotting within the peraluminous field although some samples are found to plot inside the metaluminous field. This may indicate their derivation from a magma characterized by peraluminous to metaluminous nature. Again, the overlap nature of the data points of these volcanics indicates their cogenetic origin.

The  $\text{K}_2\text{O}$ - $\text{SiO}_2$  relationship (Le Maitre 1989), ( Fig.24) indicates that most of the plotted samples lie in the high-, and medium-

K (calc-alkaline) series except three samples increase in  $\text{K}_2\text{O}$  contents therefore, they are plotted in the shoshonite field.

### Tectonic Setting Of The Studied Volcanics

The impact of the different environments on the geochemistry of their associated rock suites have been thoroughly investigated (e.g. Pearce and Cann,1973; Miyashero and shido,1975; Wood et al,1979; Pearce, 1982 and1987; Mullen,1983 and Mechede,1986).

Pearce et al. (1975) employed the  $K_2O$ - $TiO_2$ - $P_2O_5$  diagram to discriminate between the oceanic and non-oceanic basaltic rocks. On this diagram, the studied volcanic rocks plot in the non-oceanic (continental) field (Fig. 25). Using the Zr-Ti discrimination diagram of Pearce (1982) (Fig. 26) indicating that these volcanics are entirely plotted on the within-plate tectonic field. On plotting the data points of the studied volcanics on the discrimination diagram of Miyashiro and Shido (1975) which used Ni versus  $FeO/MgO$  (Fig.27), it is clear that the samples are plotting on the field of volcanic and related intrusive rocks in stable continents and oceanic islands. One sample only is plotted on the field of volcanic rocks of island -arc and active continental margins due to its lower content of Ni.

Grebennikov et al. (2013) used the molecular amounts of  $Al_2O_3/(CaO + MgO)$  VS.  $Fe_2O_{3Tot}/(CaO + MgO)$  to discriminate between the acidic volcanics evolved in different geodynamic settings. Grebennikov et al. (Op.Cit) able to distinguish between four tectonic environments in which acidic volcanics are emplaced. The first field is designated for zones of island arc and continental margin suprasubduction magmatism while the second is specified for the zone of transform plate boundaries: within\_ and marginal conti-

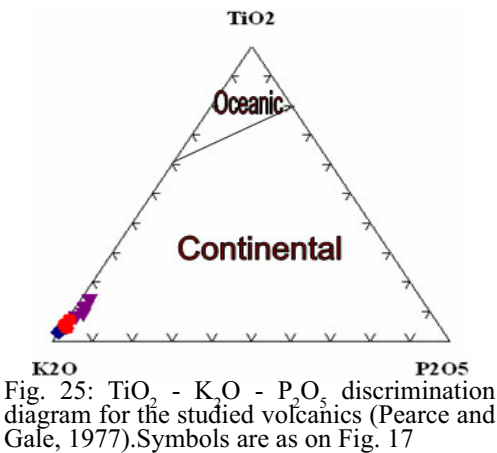


Fig. 25:  $TiO_2$  -  $K_2O$  -  $P_2O_5$  discrimination diagram for the studied volcanics (Pearce and Gale, 1977). Symbols are as on Fig. 17

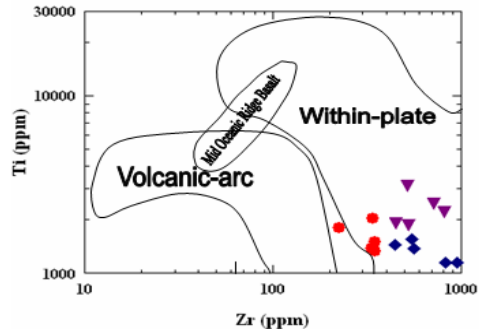


Fig. 26: Ti-Zr tectonic discrimination diagram of the studied rocks (Pearce, 1982). Symbols are as on Fig. 17

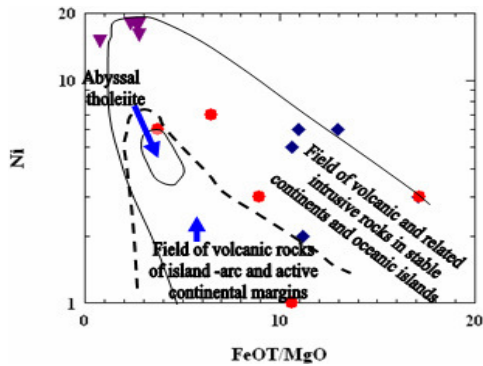


Fig. 27:  $FeO/MgO$ -Ni variation diagram for the studied volcanics (According to Miyashiro and Shido,1975); Symbols are as on Fig. 17

ental types. The third field characterizes the zones of within plate magmatism of oceanic and continental types while the fourth field is used for spreading zones. On plotting the data points of the studied volcanics on the above mentioned diagram (Fig.28), it is obvious that the data are falling within the within- plate magmatism of oceanic and continental types and spreading zones fields. The within-plate tectonic setting of the studied volcanics is also confirmed when plotting their data points on the Zr vs. Y diagram of Muller et al. (1991) differentiating between the within-plate and

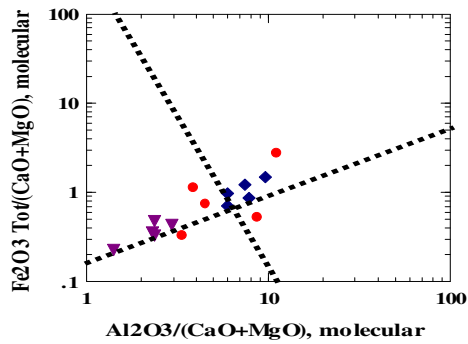


Fig. 28:  $\text{Al}_2\text{O}_3/(\text{CaO} + \text{MgO})$  VS  $\text{Fe}_2\text{O}_3\text{Tot}/(\text{CaO} + \text{MgO})$  diagram of Grebennikov et al. 2013; (I) Zones of island arc and continental margin suprasubduction magmatism; (II) Zone of transform plate boundaries: within and marginal continental types; (III) Zones of within plate magmatism of oceanic and continental types; (IV) spreading zones: rhyolites of the Galapagos Islands. Symbols are as on Fig. 17

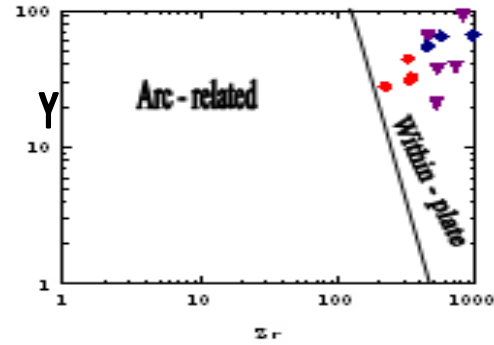


Fig. 29: Zr vs. Y diagram of Muller et al. (1992); To discriminate between within-plate and arc-related volcanic. Symbols are as on Fig. 17

arc-related volcanics. Figure (29) shows such discrimination where all the samples are plotted in the within-plate field.

In terms of testing the genetic relation between the studied rocks, the analysed samples are plotted on the  $\text{Al}_2\text{O}_3/\text{TiO}_2$  versus  $\text{TiO}_2$  of Sun and Nesbitt (1978). Figure (30) illustrates clearly that the investigated volcanics fall along a curved continuous line indicating that they might have resulted from the one magma source. Where, the  $\text{TiO}_2$ -rich magma being the least fractionated (basaltic andesite, andesite and trachy-andesite), while the  $\text{TiO}_2$ -poor magma represented the more-fractionated varieties (dacite, rhyodacites and rhyolite).

Chondrite-normalized rare-earth elements pattern of the studied volcanics is shown on Fig. (31). The rare earth elements values are normalized to chondrite values cited in Nakamura (1974). The pattern shows negative Eu anomalies that increase in extent with increasing silica content. This is a criterion for plagioclase fractionation in the rock forming

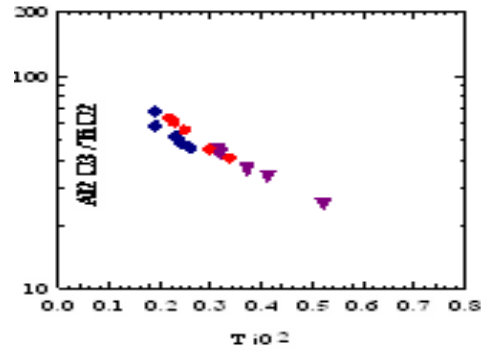


Fig. 30:  $\text{Al}_2\text{O}_3/\text{TiO}_2$  vs.  $\text{TiO}_2$  plots of the investigated volcanic (According to Sun and Nesbitt, 1978); for the studied volcanics. Symbols as on Fig. 17

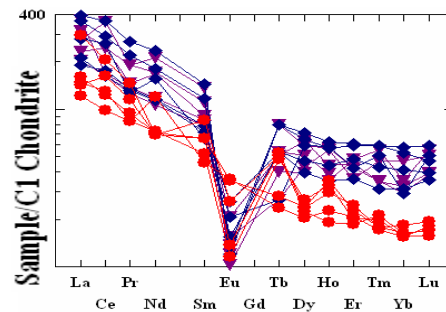


Fig. 31: Normalized pattern for REE of The studied volcanic rocks; Symbols as on Fig. 17

melt and indicates the importance of fractional crystallization in their evolution. The figure also shows an enrichment of LREE content relative to the HREE. In general, the relatively pronounced negative Eu-anomaly and enrichment in LREE/HREE in the volcanic suite indicate crystallization from a magma extremely depleted in plagioclase in its most evolved residual liquids.

Though it has long been established that the Eu-anomaly is associated with the fractionation of plagioclase. Some recent studies (Grenne and Roberts, 1998; Abdel Rahman, 1998) ascribe the presence of negative Eu anomaly to higher oxidation state (oxygen activity) of the melt that is possibly related to volatile saturation. The oxygen activity of the melt is sufficiently high to keep Eu in the trivalent state and thus preventing its incorporation into the accumulating plagioclase.

The overall enrichment in LREE relative to HREE as shown on Figure is an indication to zircon fractionation which is a common accessory mineral in these rocks.

The A-type character of the magma from which the studied volcanics were derived can be deduced by plotting their Y/Nb versus Rb/Nb ratios on Eby (1992) diagram. Although this diagram was originally used for the granitoid rocks, however, it gives clues about the character of the magma from which the rock was derived. Figure (32) shows such plotting for the studied volcanics where most of data points fall within the A2 field and few plot within the A1 field. This result is consistent with that suggested by Azer (2007) for Katharina Volcanics. Whalen et al., (1987) and Eby, (1990, 1992) stated that magma with A-type geochemical characteristics could be generated through several processes. Various petrogenetic models have been proposed for the A-type magmatism. While some authors (Bonin and Giret, 1985; Turner et al., 1992) proposed a mantle origin for A-type magmas without a significant crustal contribution based on features such as high temperature, relatively an-

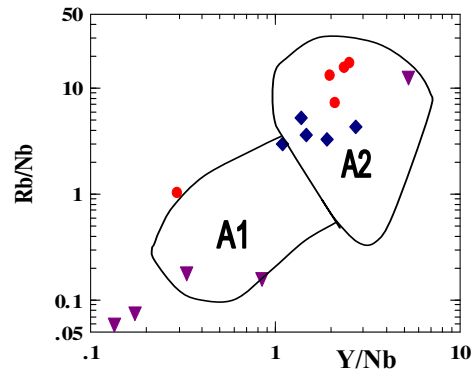


Fig. 32: Rb/Nb vs. Y/Nb diagram for distinction of A-type granitoids ( According to Eby, 1992); Symbols as on Fig.(17)

hydrous nature, and low initial  $^{87}\text{Sr}/^{86}\text{Sr}$  ratios and others (Collins et al., 1982; Chappell et al., 1987) considered the A-type suites as anatectic melts of various crustal sources such as granulitic lower crust. Landenberger and Collins, (1996) proposed that A-type magma was originated by the anatexis of charnokitic lower crust. Cullers et al., (1981) and Creaser et al., (1991) considered the anatexis of tonalitic crust as the source of such magma. Stoesser and Elliott (1980) proposed a petrogenetic model for the A-type suites involving their generation through fractionation of I-type melts, while Whalen et al. (1987) and Sylvester (1989) believe that A-type melts were derived from older rocks from which an I-type melt had been extracted earlier. The geochemical characteristics of the studied volcanics indicate that they derived from mantle source with crustal contamination. The presence of some trace elements such as Ni, Cr and V may confirm the mantle origin of these volcanics where they can be produced by differentiation from basaltic magma with some contributions from the crust. The presence of basaltic rocks in areas adjacent to the studied areas, e.g. Fierani and Wadi Kholafiya, and the presence of some trace elements such as Rb, Sr and Zr may support the above mentioned origin for these vol-

canics. The differentiation processes leading to the formation of these volcanics can also be confirmed when plotting their data points on the diagram of Gill, 1981 who used the plotting of  $\text{SiO}_2$  versus  $\text{K}_2\text{O}$  (Fig.33).

In conclusion, the studied volcanics have many geochemical characteristics of metaluminous to peraluminous A-type magma that were emplaced into within plate tectonic environment and evolved through differentiation processes from mantle-derived basaltic magma with noticeable crustal contamination. The fractionation of plagioclase in the early formed basaltic rocks leads to the pronounced negative Eu anomaly displaced by these volcanics.

#### Uranium And Thorium Distribution Of The Studied Volcanic

The two radioelements (U and Th) are measured using the gamma-ray spectrometer Gs 512 which is manufactured by Geofyzika Brno-Czech Republic. It is a digital portable instrument designed essentially for gamma-ray energy spectra measurement with 512 channel operation in range of 0.1 to 3 MeV. It is used

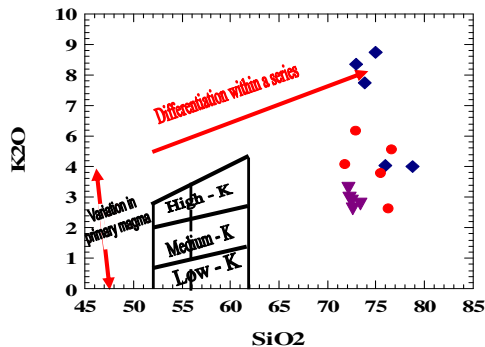


Fig. 33:  $\text{K}_2\text{O}$ - $\text{SiO}_2$  diagram distinguishing high-K, medium-K and low-K series. Differentiation within a series (presumably dominated by fractional crystallization) is indicated by the arrow. Different primary magmas (to the left) are distinguished by vertical variations in  $\text{K}_2\text{O}$  at low  $\text{SiO}_2$ . (According to Gill, 1981); Symbols as on Fig. (17).

to measure the gamma rays as total radiation counts (Tc), equivalent uranium (eU ppm), equivalent thorium (eTh ppm) and  $^{40}\text{K}\%$ . Gamma spectrometric determination of U in field conditions is indirect and carried out by the detection of  $^{214}\text{Bi}$  gamma rays, a product of  $^{238}\text{U}$  disintegration series. The obtained results are expressed in ppm eU (equivalent uranium concentration). Gamma spectrometric determination of Th in field conditions is also indirect and can be realized by detection of  $^{208}\text{Tl}$  gamma rays, a product of  $^{232}\text{Th}$  disintegration series. The results are also expressed in ppm eTh (equivalent thorium concentration). Gamma ray spectrometers record also gamma rays, as total count (Geofyzika Brno, 1998).

Felsic volcanics constitute a primary source of uranium for forming an economic deposit. The significance of acid volcanic rocks as a potential uranium source lies in the readily leachable form of their uranium content. Among the acid volcanics, rhyolites form an ideal source followed by welded tuffs, ignimbrites, etc. The alkali rhyolite is generally ideal for its enrichment in many lithophile elements including uranium, which are amenable to subsequent leaching by meteoric water. Observations of the behavior of uranium and thorium during the formation of igneous rocks indicate higher concentrations in the youngest and most felsic and silicic members. Volcanic rocks, especially the felsic variety are often found to be richer in uranium and thorium than their plutonic equivalents, with earlier eruptions showing highest concentrations.

Uranium in volcanic rocks is bound in the matrix making them easily separable, which is a prerequisite in the uranium ore forming process. The felsic volcanic rocks, viz. rhyolite, rhyodacite and dacite have uranium contents higher than the crustal average, due to magmatic segregation. Klepper and Wyand (1956) cite a study showing that the volcanic rocks are often 1.5 to 2 times higher in uranium content than their intrusive equivalents. Four modes of occurrence of uranium in volcanic rocks are

proposed by Zielinsky (1981) namely; 1) uranium occurs as uraniferous accessory mineral (e.g. zircon, sphene, apatite); 2) occurs in secondary oxide of iron manganese (or) titanium; 3) occurs in volcanic glass and 4) at mineral grain boundaries.

In rhyolites, the largest share of whole rock uranium is often contained in volcanic glass, which is readily removed by glass water interactions. Such rhyolitic rocks can be a good source of uranium for secondary uranium mineralization, which can occur along fractures, bedding planes, porous and permeable zones, organic rich units either within the volcanics (or) in adjoining rock units. Uranium can also be released from volcanic glass shards, by solution activity (Walton et. al. 1979 )

The measured uranium and Thorium contents of the studied volcanics are presented in Table (3). It is noticed that Ras Naqab volcanics have the highest U and Th contents that ranging from 3 to 37 ppm for U and from 12 to 24 ppm for Th with an average 15 ppm and 17 ppm, respectively. Umm Shouki volcanics (5 to 17 ppm U and 13 to 22 ppm Th) come in the second order of abundance while Iqna Sharaya volcanics (aver. U and Th, 8.5 and 16.7 ppm respectively) have the latest contents of the two radioelements (Table 3). The studied volcanics are considered to be an important source rock of uranium, since

they contain more than 7 ppm U. The acidic volcanics that contain 7 ppm U and 20 to 30 ppm Th are considered by many authors as an important source of uranium (Rosholt and co-workers, 1969, 1971; Shatkov et al. 1970; and Zielinski and co-workers, 1977, 1978, 1980).

In order to understand the behaviour of the two radioelements during the course of magmatic evolution of the studied volcanics, their contents must be portrayed on some variation diagrams (Figs.34 -36). It is well known that the Th: U ratio is 3:1 in magmatic derived rocks. If this ratio is disturbed, a post magmatic processes of uranium depletion and/or enrichment may be expected to occur. In this case, however, uranium ratio is expected to be changed because of its high mobility compared with thorium. Figure (34) shows the plotting of U versus Th of the Ras Naqab volcanics where no magmatic control affecting the behaviour of the two radioelements. Instead, processes of uranium depletion and enrichments are expected to occur as indicated from the values of the Th/U ratio that ranging between 0.54 and 4.7 (Table 3).

The uranium is leached in some places, by the effect of solutions mainly meteoric water and hydrothermal solutions, and precipitated in other suitable environment within the same volcanic pluton. This environment is mainly occurred in the alteration zones where feldspars

Table 3 : U and Th contents of the studied volcanics

	NQ1	NQ2	NQ3	NQ4	NQ5	NQ6	NQ7	NQ8	NQ9	NQ10	Aver.
<b>Ras Naqab Rhyolite</b>											
Th	17	12	13	21	16	12	14	23	18	24	17
U	4	5	3	39	4	6	3	37	28	22	15.1
U/Th	0.24	0.42	0.23	1.86	0.25	0.5	0.21	1.61	1.56	0.92	0.788
Th/U	4.25	2.4	4.3	0.54	4	2	4.7	0.62	0.64	1.1	1.13
<b>Iqna Sharaya volcanics</b>											
	IS1	IS2	IS3	IS4	IS5	IS6	IS7	IS8	IS9	IS10	Aver.
Th	13	14	11	12	15	17	19	21	25	20	16.7
U	5	7	6	4	5	13	12	15	10	8	8.5
U/Th	0.38	0.5	0.55	0.33	0.33	0.76	0.63	0.71	0.40	0.40	0.499
Th/U	2.6	2	1.83	3	3	1.31	1.58	1.4	2.5	2.5	1.96
<b>Umm Shouki volcanics</b>											
	USH1	USH2	USH3	USH4	USH5	USH6	USH7	USH8	USH9	USH10	Aver.
Th	15	14	18	13	14	19	15	22	17	22	16.9
U	7	6	9	5	6	7	11	17	8	10	8.6
U/Th	0.47	0.43	0.50	0.38	0.43	0.37	0.73	0.77	0.47	0.45	0.51
Th/U	2.14	2.33	2	2.6	2.33	2.71	1.36	1.29	2.13	2.2	1.97

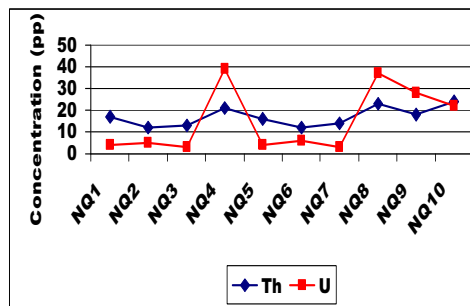


Fig.34:U vs Th diagram of the studied volcanic, Ras Naqab

are generally altered to sericite and koalenitic materials, as confirmed by the petrographic examinations, where uranium is generally adsorbed along the grain boundary of either feldspars and their alteration products. Other environment is also suggested to occur at the zones of biotite alteration and the liberation of iron oxides along its cleavage planes. However, the higher U concentrations can be partly explained by the abundance of Fe-Ti-Mn oxides with a greater density of possible precipitation sites for U. Furthermore, the greater permeability and porosity of these horizons contributed to the high degree of hydrothermal alteration, and hence U enrichment associated with sericite.

The behaviour of U and Th within the studied volcanics at both of Iqna Sharaya and Umm Shouki areas is illustrated on Figs. (35&36). The figures show the positive correlation between the two elements to suggest the magmatic control on their behaviour where these elements may incorporate within some accessory minerals such as zircon and monazite. The role of the post magmatic processes on these two elements cannot be neglected.

#### Mode Of Occurrence Of The U And Th In The Studied Volcanics

The uranium in volcanic rocks generally has three modes of occurrences: (1) as par-

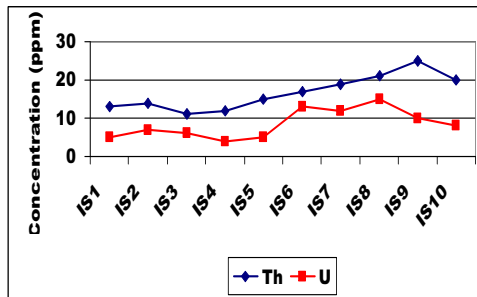


Fig.35: U vs Th diagram of the studied volcanic, Iqna Sharay'a

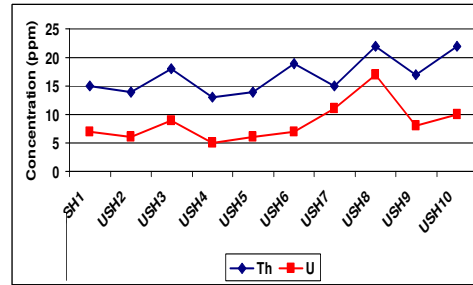


Fig.36: U vs Th diagram of the studied volcanic, Umm Shouki

ticles scattered uniformly throughout the volcanic matrices; (2) as particles adsorbed on ferrooxides, altered minerals, microfissures in minerals or along grain boundaries; (3) or as micro-uranium minerals and uranium-bearing accessory minerals. The uranium occurred in the first two modes are easily mobilized through deuteric and/or hydrothermal alteration while that included in accessory minerals is dissolved through high temperatures along the shear zones.

The U and Th contents of the studied volcanics are graphically represented ( Figs.37,38 &39) where three assumptions of uranium behavior are inferred. The first one assumes that in some samples, (marked with blue star), thorium is mainly three times more abundant than uranium which means that the two elements are magmatically controlled and should be incorporated in accessory minerals such as zircon, monazite and uranothorite. In the second case, uranium is equal to one half of the thorium or slightly more indicating that a process of uranium enrichment (U-gain as marked with red circles) may be occurred. In this case, uranium is adsorbed on ferrooxides, altered minerals, microfissures in minerals or along grain boundaries. When uranium is less than one quarter of thorium or completely disappear, a process of uranium leaching (U-loss as marked with crossed circles) may take place.

In Ras Naqab Volcanics, the previously mentioned three modes of occurrence of uranium and thorium are represented (Fig. 37) where uranium is leached by the effect of the circulating meteoric and hydrothermal solutions and later reprecipitated in the altered zones present in the same volcanic pluton. The volcanics outcropped in the other two areas (i.e. Umm Shouki and Iqna Sharaya) have only two modes of occurrence of the two elements (Fig. 38&39) (i.e. uranium enrichment and U & Th - bearing accessory minerals).

**U And Th-bearing Minerals Present In The Studied Volcanics**

For studying U and Th-bearing minerals present in the studied volcanics, 10 representative samples are collected, crushed using jaw crushers, sieved using sieves (60-30 mesh), and subjected to heavy liquids separation using bromoform and methylene iodide. The obtained light and heavy fractions of methylene iodide were subjected to the magnetic separation methods and a subsequent hand picking operations were carried out. The picked grains of minerals were prepared for scan electron microscope (ESEM-EDAX) investigations to determine their main constituents. The following is the description of the examined minerals

For studying U and Th-bearing minerals present in the studied volcanics, 10 representative samples are collected, crushed using jaw crushers, sieved using sieves (60-30 mesh), and subjected to heavy liquids separation using bromoform and methylene iodide. The obtained light and heavy fractions of methylene iodide were subjected to the magnetic separation methods and a subsequent hand picking operations were carried out. The picked grains of minerals were prepared for scan electron microscope (ESEM-EDX) investigations to determine their main constituents. The following is the description of the examined minerals;

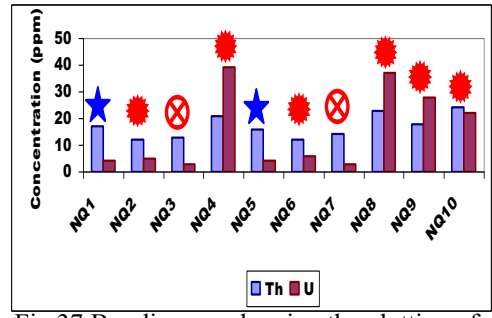


Fig.37: Bar diagram showing the plotting of U and Th in the studied Ras Naqab volcanic. ★ Uranium loss; ★ Uranium gain; ★ Magmatic control

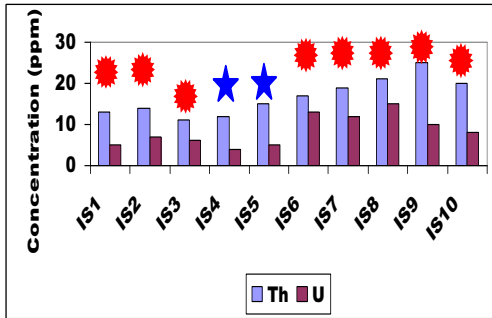


Fig.38 Bar diagram showing the plotting of U and Th in the studied Iqna Sharaya volcanic, symbols as on Fig.37

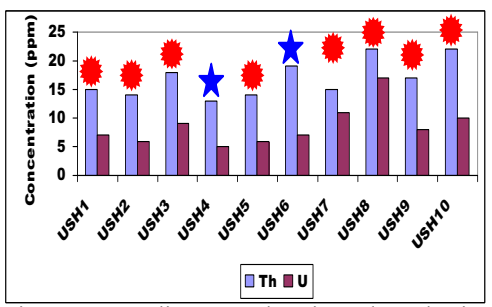


Fig.39: Bar diagram showing the plotting of U and Th in the studied Umm Shouki volcanic, symbols as on Fig.37

### Zircon ( $ZrSiO_4$ )

Zircon crystals have euhedral prismatic form with brown and reddish brown colour and have adamantine and resinous luster. Zircon is generally surrounded with pleochroic halos due to radiation effects. Most of the examined zircon crystals in both Iqna Sharaya and Umm Shouki areas are metamict. The metamict zircon is highly radioactive due to the presence of uranium and /or thorium in their structures which on turn are destructed as result of energy dissipation during the decay of the radioactive elements.

The EDX analyses (Fig. 40) show different contents of Hf, U and Th.  $HfO_2$  may be enriched in zircon reaching up to 2.5 % and  $UO_2$  may reach 4.0 %, while  $ThO_2$  exceeds 4.0 % in many crystals.

### Monazite

Monazite crystals are rare and recorded in Umm Shouki and Ras Naqab volcanics. The EDX analyses (Fig. 41) indicate that monazite is a phosphate of rare earth metals (Ce and La)  $PO_4$  with considerable  $ThO_2$  content that attains 4.7 % and relatively lesser content of  $UO_2$  reaching about 0.82 wt. %. Most of examined monazite grains are small in size (200 to 350  $\mu m$ ) and have elongated prismatic form with yellowish to reddish brown colour.

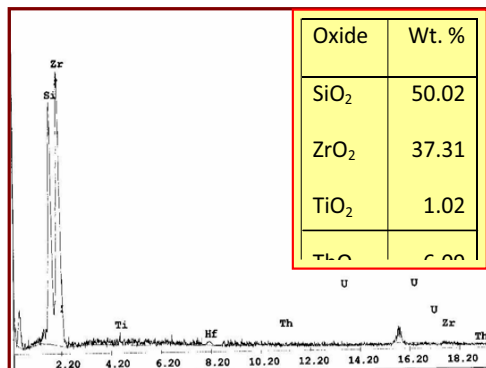


Fig.40: ESEM-EDAX analysis of zircon

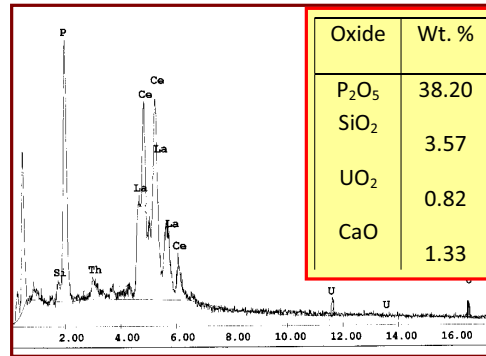


Fig.41: ESEM-EDAX analysis of monazite

### Uranothorite

Uranothorite generally contains up to 10%U and  $ThO_2$  from 49% to 75% (Aswathanarayana, 1985 and Heinrich, 1958). The authors (Op. Cit) mentioned that other element associations are commonly present in small amounts such as Ca, Mg,  $Fe^{2+}$ , alkalis, Ce earths, P, Ta, Ti, Zr, Sn, Al and Y-elements may occur Pb and  $Fe^{3+}$  may be abundant (Ferrothorite).

In the studied Ras Naqab volcanics, the uranothorite occurs as anhedral to subhedral light brown crystals. They show a normal distribution of U, Ti, Fe, Y and Ca. Si is relatively high (20.70%) while Th has low value (25.62%). This may be due to substitution of Th by Si. It is noticed that the uranothorite contains a considerable amounts of REE such as Ce, Nd and Sm.. Two possible interpretations are proposed for this phenomenon. The first assumes the presence of REE-bearing inclusions within the uranothorite. The second interpretation assumes that the studied uranothorite is considered as an alteration products of monazite. The writer inclined to the first opinion where the analyses of the uranothorite illustrated on Fig. (42) show no phosphorous which is essential constituent in monazite.

### Tornebohmite

Tornebohmite  $(Ce,La,Nd)_2Al(SiO_4)_2(OH)$

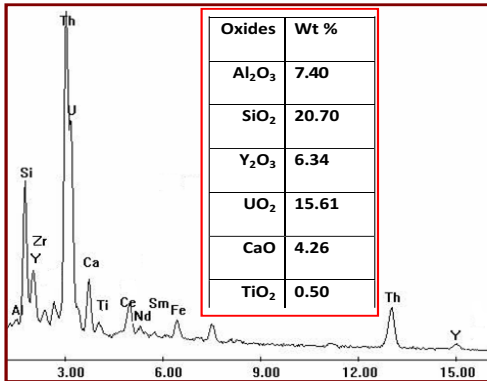


Fig.42: ESEM-EDAX analysis of uranothorite

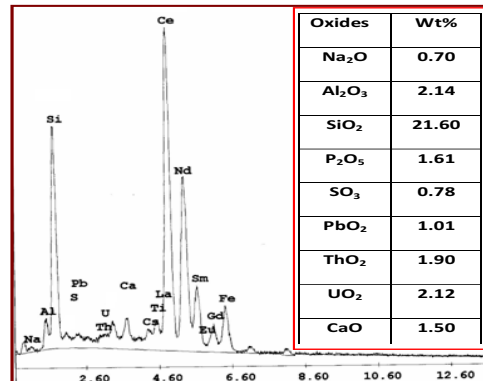


Fig.43: ESEM-EDAX analysis of tornebohmite

is a U & Th- bearing rare earth mineral. Tornebohmite is classified, based on the presence of either Ce or La, into tornebohmite-Ce or tornebohmite-La respectively. Generally, the weight percentages of La<sub>2</sub>O<sub>3</sub>, Ce<sub>2</sub>O<sub>3</sub>, Al<sub>2</sub>O<sub>3</sub>, Nd<sub>2</sub>O<sub>3</sub> and SiO<sub>2</sub> recorded in tornebohmite are 16.00%, 38.69 %, 10.02 %, 9.92 % and 23.61 % respectively (Shen and Moore, 1982). The mineral is distinguished by its green colour, vitreous to adamantine luster. Tornebohmite is recorded as a radioactive mineral as defined in 49 CFR (Code of Federal Regulations) 173.403.

The studied tornebohmite can be classified as Ce-bearing variety as indicated from the ESEM analysis shown on Fig. (43) where it enriched in Ce (Ce<sub>2</sub>O<sub>3</sub> = 39.30 wt%). The majority of the analysed REE have low concentrations where La<sub>2</sub>O<sub>3</sub>, Sm<sub>2</sub>O<sub>3</sub>, Eu<sub>2</sub>O<sub>3</sub> and Gd<sub>2</sub>O<sub>3</sub> reaching 0.60 wt %, 1.06 wt %, 1.52 wt % and 1.00 wt % respectively. It also contains considerable amounts of U and Th oxides (2.12 wt% and 1.90 wt% respectively). Abnormal content of Nd<sub>2</sub>O<sub>3</sub> is recorded (16.20 wt%). content of Nd<sub>2</sub>O<sub>3</sub> is recorded (16.20 wt%).

Tornebohmite is considered as an important REE-bearing mineral which has been found in hydrothermal environments (Staatz, 1985; Oreskes and Einaudi, 1992 and Negwenya, 1994). Furthermore, Cerium, as the main constituent in tornebohmite, was early record-

ed in metasomatic rocks at Bastnas, Sweden (Shen and Moore, 1982). The hydrothermal system is defined by Williams et al. (Op.Cit) to be any system in which heated aqueous solutions interact with rocks or melts. Accordingly, hydrothermal fluids are not restricted to direct or indirect involvement of igneous rocks or melts. Beside tornebohmite, other less important RE minerals are formed in hydrothermal environments e.g. ancylite, branerite, davidite, thorite, (Staatz, 1985; Oreskes and Einaudi, 1992 and Negwenya, 1994). In many localities, the hydrothermally formed RE minerals are associated with apatite and fluorite which are both usually rich in REE.

The hydrothermally-formed RE minerals are recorded in various geologic settings ranging from fracture- fillings and breccias to veins, stockworks, skarns and large scale metasomatic replacement bodies. Some U-REE skarn in Queensland (Australia) was formed by fluids derived from a nearby granite intrusion (Kwak and Abeysinghe, 1987)

On the scope of the foregoing discussion, the investigated tornebohmite may be formed by hydrothermal fluids through the fracture system penetrating the studied volcanics. These fluids may be accompanied and contemporaneous with the syenogranite magma that intruded the volcanic rocks outcropping at Wadi Kholyfia at the southwestern part of

Ras Naqab area.

### CONCLUSION

The detailed studies that carried out on the selected acidic volcanics exposed at Ras Naqab, Iqna Sharaya and Umm Shouki areas reveal that they have many geochemical characteristics of metaluminous to peraluminous A-type magma that were emplaced into within plate tectonic environment and evolved through differentiation processes from mantle-derived basaltic magma with noticeable crustal contamination. The fractionation of plagioclase in the early formed basaltic rocks leads to the pronounced negative Eu anomaly displaced by these volcanics. These volcanic rocks are represented mainly with lava flows of rhyolitic composition, lithic and crystal tuffs.

They considered as source for uranium since they contain more than 8 ppm average uranium content. The average thorium and uranium contents are 17ppm and 15 ppm for Ras Naqab volcanics, 16.7 ppm and 8.5 ppm for Iqna Sharaya while Umm Shouki volcanics have 17 ppm average Th and 8.6 ppm average U.

Three assumptions of uranium behaviour are inferred. The first one assumes that in some samples, thorium is mainly three times more abundant than uranium which means that the two elements are magmatically controlled and should be incorporated in accessory minerals such as zircon, monazite and uranothorite and tornebohmitite. In the second case, uranium is equal to one half of the thorium or slightly more which indicates that a process of uranium enrichment (U-gain) may be occurred. In this case, uranium is adsorbed on ferroxides, altered minerals, microfissures in minerals or along grain boundaries. When uranium is less than one quarter of thorium or completely disappear, a process of uranium leaching (U-loss) may take place.

Zircon, Monazite, uranothorite and tor-

nebohmitite minerals are analysed and identified by ESEM. Also, the U&Th-bearing rare earth mineral tornebohmitite is classified as tornebohmitite-Ce where its Ce content is 39.40 wt %. Tornebohmitite may be formed by hydrothermal fluids penetrating the studied volcanics. These fluids may be accompanied and contemporaneous with the syenogranite intrusion which occurs at the southwestern part of Ras Naqab area.

### REFERENCES

- Abdel-Rahman, A. M., and Doig, R., 1987. The Rb-Sr geochronological evolution of the Ras Gharib segment of the northern Nubian shield. *J. Geol. Soc. London*, 144, 577-586.
- Abdel-Rahman, E. M., 1998. Geochemistry of mantle-related intermediate rocks from the Tibbit Hill volcanic suite, Quebec Appalachians. *Mineral. Magazine*, 62 (4), 487-500.
- Abu El-Leil, I.; Hassan, M. M.; Abd El-Tawab, M. M., and Abd El-Rahman, H. B., 1990. Geological and geochemical studies on the Feirani Group; The proposed late Proterozoic younger volcanic rocks, Sinai, Egypt. *Egypt. Mineralogist*, 2, 61-80.
- Agron, N., and Bendor, Y.K., 1981. The volcanic massif of Biq'at Hayareah (Sinai-Negev): A case of potassium metasomatism. *J. Geol.*, 89, 479 - 495.
- Agron, N., and Bendor, Y. K., 1981. The volcanic massif of Biqat Hayareah (Sinai- Negev); a case of potassium metasomatism. *J. Geol.*, 89, 479 - 496.
- Ahmed, A. M., 1985. Geological studies of some granitic rocks around Wadi Um Adawi, South-eastern Sinai, Egypt. Ph.D. Thesis, Al-Azhar Univ. Cairo, Egypt, 164p.
- Aswathanarayana, U., 1985. Principles of Nuclear Geology. Oxonian Press VT. LTD, New Delhi, India. ,397p.
- Azab, M. S., 2002. Geology, Geochemistry and

- Radioactivity of Wadi El – Morakh Basement Rocks, South Taba, Sinai, Egypt. Ph. D. Thesis, Suez Canal Univ. Ismailia, Egypt. 206p.
- Azer, K., 2007. Tectonic significance of Late Precambrian calc-alkaline and alkaline magmatism in Saint Katherina Area, Southern Sinai, Egypt. *Geologica Acta: an Inter. Earth Science J.*, 5, núm. 3, 255- 272.
- Bentor, Y.K., 1985. The crustal evolution of the Arabo-Nubian massif with special reference to the Sinai Peninsula. *Precamb. Res.*, 1-74.
- Bentor, Y. K., and Eyal, M., 1987. The geology of Sinai, its implication for the evolution of the Arabo-Nubian Massif, Jebel Sabbagh sheet. *The Israel Acad. Sci. and Humanities*, 484 p.
- Bielski, M., 1982. Stages in evaluation of the Arabian-Nubian Massif in Sinai, Ph. D. Thesis, Hebrew Univ., Jerusalem, 155 p.
- Black, R., and Liegeois, J. P., 1993. Cratons, mobile belts, alkaline rocks and continental lithospheric mantle; the Pan-African testimony. *J. Geol. Soc. London*, 150, 89–98.
- Bonin, B., and Giret, A., 1985. Contrasting roles of rock-forming minerals in alkaline ring complexes. *J. Afri. Earth Sci.*, 3, 41-49.
- Chappell, B.W.; White, A. J. R., and Wyborn, D., 1987. The importance of residual source material (restite) in granite petrogenesis. *J. Petrol.*, 28, 1111-1138.
- Collins, W. J.; Beams, S.D.; White, A. J. R., and Chappell, B.W., 1982. Nature and origin of A-type granites with particular reference to southeastern Australia. *Contrib. Mineral. and Petrol.*, 80, 189-200.
- Cox, K. G.; Bell, J. D., and Pankhurst, R. J., 1979. *The Interpretation of Igneous Rocks*. Allen and Unwin, London, 450 p.
- Creaser, R. A.; Price, R. C., and Wormald, R. J., 1991. A-type granites revisited: Assessment of a residual-source model. *Geology*, 19, 163-166.
- Cullers, R. L.; Koch, R. J., and Bickford, M. E., 1981. Chemical evolution of magmas in the Proterozoic terrane of the St. Francois Mountains, southeastern Missouri. *J. Geophysical Res.*, 86, 10388-10401.
- Donaldson, C. H., and Henderson, C. M. B., 1988. A new interpretation of round embayments in quartz crystals. *Min. Mag.*, 52, 27 – 33.
- Eby, G. N., 1990. The A-type granitoids: A review of their occurrence and chemical characteristics and speculations on their petrogenesis. *Lithos*, 26, 115-134.
- Eby, G. N., 1992. Chemical subdivision of the A-type granitoids: Petrogenetic and tectonic implications. *Geology*, 20, 641-644.
- Egyptian Geological Survey and Mining Authority, EGSM, 1981. Geologic map of Egypt. Scale 1: 200,000. Egypt. Geol. Surv. Egypt, Cairo, 1 map.
- Eissa, M. M. E., 2000. Geology and mineralization of southern Sinai-Egypt between lat. 33°20' – 33°45' E. Ph. D. Thesis, Zagazig Univ., Zagazig, Egypt, 220p.
- El Masry, N. N., 1991. Geological studies of paleovolcanics and volcanoclastics of Sainte Catherine mountain area, southern Sinai, Egypt. M. Sc. Thesis. Suez Canal Univ. Ismailia, Egypt, 87p.
- El Masry, N. N., 1998. Geology of extrusive and intrusive rocks of Feirani area, southern Sinai, Egypt. Ph.D Thesis. Suez Canal Univ. Ismailia, Egypt. 206p.
- El Sayed, A. A., 1993. Geology and radioactivity of west Dahab area, southern Sinai, Egypt. M.Sc Thesis. Mansoura Univ. Mansoura, Egypt, 201p.
- El-Gaby, S.; Khudeir, A. A., and El-Taky, M., 1989. The Dokhan Volcanics at Wadi Queh area, Central Eastern Desert, Egypt. 1<sup>st</sup> Conf. Geochemistry, Alexandria Univ., Egypt, 42–62.
- El-Gaby, S.; Khudier, A. A.; Abdel Tawab, M., and Atalla, R.F., 1991. The metamorphosed volcano-sedimentary succession of Wadi Kid, south-

- eastern Sinai, Egypt. *Annal. Geol. Surv. Egypt*, XVII, 19–35.
- El-Gaby, S.; List, F. K., and Tehrani, R., 1988. Geology, evolution and metallogenesis of the Pan-African Belt in Egypt. In: *The Pan-African Belt of Northeast Africa and Adjacent areas* (El-Gaby, S.; Greiling, R.O., Eds.). Braunschweig Viewig, 17–68.
- El-Gaby, S.; List, F. K., and Tehrani, R., 1990. The basement complex of the Eastern Desert and Sinai. In: *The geology of Egypt* (Said R., Ed.). Rotterdam, A.A. Balkema, 175-184.
- El-Gammal, S. A. S., 1986. Geology of the granitoid rocks of the northwestern part of the basement rocks in Sinai, Egypt. Ph.D. Thesis, Al-Azhar Univ. Cairo, Egypt. 252 p.
- El-Masry, N. N.; El-Kaliouby, B. A.; Khawasik, S. M., and El-Ghawaby, M. A., 1992. Reconsideration of the geologic evolution of Saint Catherine ring dyke, South Sinai, Egypt. 3<sup>rd</sup> Conf. Geol. Sinai Develop., Ismailia, Egypt, 229–238.
- El-Metwally, A. A., 1997. Petrogenesis of gabbroic rock intrusions from south-Central Sinai massif. A transition from arc to intraplate magmatism. 3<sup>rd</sup> Conf. Geochem. Alex. Univ. (1).
- El-Morsy, D. M., 1988. Geology, petrology and geochemistry of the Sinai Katrina mountains, southern Sinai, Egypt. M.Sc. Thesis, Kuwait Univ. Kuwait. 184 p.
- El-Reedy, M. W., 1984. The general physical and chemical features and the pollution level of El-Sabahia – Sabhan – El-Reqa soil localities State of Kuwait. Inter. Report Environment Protection Dept. Ministry of Pub. Health, El-Kuwait ( Part. 1 : Chemical methods ), 10.
- Eyal, M.; Bartov, Y.; Shimron, A. E., and Bentor, Y.K., 1980. Sinai Geological Map, Scale 1: 500 000. Geological Survey of Israel.
- Eyal, M., and Hezkiyahu, T., 1980. Katherina pluton: the outline of a petrologic framework. *Israel J. Earth Sci.*, 29, 41-52.
- Garfunkel, Z., 1999. History and paleogeography during the Pan-African orogen to stable platform transition: Reappraisal of the evidence from the Elat area and the northern Arabian-Nubian Shield: *Isr. J. Earth Sci.*, 48, 135-157.
- Gass, I. G., 1982. Upper Proterozoic (Pan-African) calc-alkaline magmatism in northeastern Africa and Arabia. In: *Orogenic Andesites and Related Rocks* (Thorpe, R.S., Ed.). Wiley, New York, 591–609.
- Geofyzika Brno, 1998. Portable Gamma-Ray Spectrometer GS-512. Instruction Manual, Version 2.00, Brno, Czech Republic, 78 p.
- Ghoneim, M. F.; Aly, S. M., and El-Baraga, M. H., 1989. Geochemistry of the Melheg metavolcanics, south Sinai Peninsula, Egypt. *Ann. Geol. Surv. Egypt.*, 15, 171-182.
- Gill, J. B., 1981. *Orogenic andesites and plate tectonics*. Berlin, Springer-Verlag, 358 p.
- Grebennikov, A. V.; Popov, V. K., and Khanchuk, A. I., 2013. Experience of Petrochemical Typification of Acid Volcanic Rocks from Different Geodynamic Settings. *Russian J. Pacific Geol.*, 7, No. 3, 212–216.
- Grenne, T., and Roberts, D., 1998. The Holonda porphyrites, Norwegian Caledonides: Geochemistry and tectonic setting of Early-Mid-Ordovician shoshonitic volcanism. *J. Geol. Soc. London*, 155, 131-142.
- Harris, N. B. W.; Hawkesworth, C. J., and Ries, A. C., 1984. Crustal evolution in northeast and east Africa from model Nd ages. *Nature*, 309, 773–776.
- Heinrich, E. W., 1958. *Mineralogy and geology of radioactive raw materials*, McGraw Hill, New York-Toronto-London, 654p.
- Irvine, T. N., and Baragar, W. R. A., 1971. A guide to the chemical classification of the common volcanic rocks. *Can. Jour. Earth Science*, 8, 523-548.
- Jarrar, G.; Stern, R. J.; Saffarini, G., and Al-Zubi, H., 2003. Late- and post-orogenic Neopro-

- terozoic intrusions of Jordan: implications for crustal growth in the northernmost segment of the East African orogen. *Precam. Res.*, 123, 295–319.
- Jarrar, G. H.; Mntona, W. I.; Stern, R. J., and Zachmann, F., 2008. Late Neoproterozoic A-type granites in the northernmost Arabian-Nubian Shield formed by fractionation of basaltic melts. *Chemie der Erde*, 68, 295–312.
- Katzir, Y.; Litvinovsky, B. A.; Jahn, B. M.; Eyal, M.; Zanzvilevich, A. N.; Valley, J. W.; Vapnik, Ye.; Beeri, Y., and Spicuzza, M. J., 2007b. Interrelations between coeval mafic and A-type silicic magmas from composite dykes in a bimodal suite of southern Israel, northernmost Arabian-Nubian Shield: geochemical and isotope constraints. *Lithos*, 97, 336–364.
- Khalaf, I. M.; Ahmed, A. M., and Seweifi, B. M., 1994. The granitoids of Ras Muhammad area, south Sinai, Egypt. *Egypt. J. Geol.*, 38 (1), 125-139.
- Klepper, and Wyand, 1956. Uranium in volcanic rocks. *Econ. Geol.*, 66, 1061-9.
- Kröner, A., 1984. Late Precambrian plate tectonics and orogeny: a need to redefine the term Pan-African. In: *African Geology* (Klerkx, J., Michot, J., Eds.). Teruren, 23–26.
- Kröner, A., 1985. Ophiolites and the evolution of tectonic boundaries in the Late Proterozoic Arabian-Nubian Shield of Northeast Africa and Arabia, *Precam. Res.*, 27, 227-300.
- Kröner, A.; Stern, R. J.; Linnabacker, P.; Manton, W.; Reischmann, T., and Hussein, I.M., 1990. Evolution of Pan-African island arc assemblages in the south Red Sea Hills, Sudan, and in SW Arabia as exemplified by geochemistry and geochronology. *Precambrian Research*, 53, 99–118.
- Kwak, T. A., and Abeyasinghe, P. B., 1987. Rare earth and uranium minerals present as daughter crystals in fluid inclusions, Mary Kathleen U-REE skarn, Queensland, Australia. *Mineral. Mag.*, 51, 665-70.
- Landenberger, B., and Collins, W. J., 1996. Derivation of A-type granites from a dehydrated charnockitic lower crust: evidence from the Chaelundi Complex, Eastern Australia. *J. Petrol.*, 37, 145–170.
- Le Maitre, R. W.; Bateman, P.; Dudek, A.; Keller, J.; Lameyre, J.; Le Bas, M. J.; Sabine, P. A.; Schmid, R.; Sorensen, H.; Streckeisen, A.; Woolley, A.R., and Zanettin, B., 1989. A classification of igneous rocks and glossary of terms. Recommendations Inter. Union Geol. Sci. Subcommission on the Systematics of Igneous Rocks. Oxford, Blackwell, 193 p.
- Lofgren, G. E., 1974. An experimental study of plagioclase crystal morphology : Isothermal crystallization. *Amer. J. Sci.*, 274, 243 – 273.
- Maniar, P. D., and Piccoli, P. M., 1989. Tectonic discrimination of granitoids. *Geol. Soc. Am. Bull.*, 101, 653-643.
- Meschede, M., 1986. A method of discriminating between different types of Mid-Ocean Ridge basalts and continental tholeiites with the Nb-Zr-Y diagram. *Chem. Geol.*, 56, 207-218.
- Miyashiro, A., and Shido, F., 1975. Tholeiitic and calcalkalic series in relation to the behaviours of titanium, vanadium, chromium and nickel. *Am. J. Sci.*, 275, 265-277.
- Moghazi, A. M., 2002. Petrology and geochemistry of Pan-African granitoids, Kab Amiri area, Egypt: Implications for tectono-magmatic stages in the Arabian–Nubian Shield evolution. *Mineral. Petrol.*, 75, 41–67.
- Moghazi, A. M.; Andersen, T.; Oweiss, G. A., and El Bouseily, A. M., 1998. Geochemical and Sr–Nd–Pb isotopic data bearing on the origin of Pan-African granitoids in the Kid area, south-east Sinai, Egypt. *J. Geol. Soc. London*, 155, 697–710.
- Moussa, H. E., 2003. Geologic setting, petrography and geochemistry of the volcano-sedimentary succession at Gebel Ferani area, southeastern Sinai, Egypt. *Egypt. J. Geol.*, 47, 153–173.

- Mullen, E. D., 1983. MnO/TiO<sub>2</sub>/P<sub>2</sub>O<sub>5</sub>: A minor element discriminates for petrogenesis. *Earth Planet. Sci. Lett.*, 62, 53-62.
- Muller, D.; Rock, N.M.S., and Groves, D.I., 1992. Geochemical discriminations between shoshonitic and potassic volcanic rocks from different tectonic settings; a pilot study: *Mineralogy and Petrology*, 46, 259-289.
- Mushkin, A.; Navon, O.; Halicz, L.; Heimann, A.; Woerner, G., and Stein, M., 1999. Geology and geochronology of the Amram Massif, southern Negev Desert, Israel. *Israel J. Earth Sci.*, 48, 179-193.
- Nakamura, N., 1974. Determination of REE, Ba, Fe, Mg, Na and K in carbonaceous and ordinary chondrites. *Geochim. Cosmochim. Acta.*, 38, 757-775.
- Negwenya, B. T., 1994. Hydrothermal rare earth mineralization in carbonatites of the Tundulu complex, Malawi: processes at the fluid/rock interface. *Geochem. Cosmochem. Acta*, 58, 2061-72.
- Oreskes, N., and Einaudi, M. T., 1992. Origin of hydrothermal fluids at Olympic Dam: preliminary results from fluid inclusions and stable isotopes. *Econ. Geol.*, 87, 64-90.
- Pearce, J. A., 1982. Trace element characteristic of lava from destructive plate boundaries. In: *andesites* (Thrope, R. S., Ed.). Wiley, Chichester, 525-548.
- Pearce, J. A., 1987. An expert system for the tectonic characterization of ancient volcanic rocks. *J. Volc. geoth. Res.*, 32, 51-65.
- Pearce, J. A., and Cann, J.R., 1973. Tectonic setting of basic volcanic rocks determined using trace element analyses. *Earth Planet. Sci. Lett.*, 19, 290-300.
- Pearce, J. A.; Gorman, B.E., and Birkett, J. C., (1975). The TiO<sub>2</sub> -K<sub>2</sub>O-P<sub>2</sub>O<sub>5</sub> diagram; a method of discriminating between oceanic and non-oceanic basalts. *Earth Planet. Sci. Lett.*, 24, 419-426.
- Ressetar, R., and Monrad, J. R., 1983. Chemical composition and tectonic setting of the Dokhan Volcanic Formation, Eastern Desert, Egypt. *J. Afr. Earth Sci.*, 1, 103-112.
- Rosholt, J. N., and Noble, D. C., 1969. *Earth. Planet. Sci. Lett.*, 6, 268-70.
- Rosholt, J. N.; Prijana, P., and Noble, D. S., 1971. *Econ. Geol.*, 66, 1061-9.
- Samuel, M. D.; Moussa, H. E., and Azer, M. K., 2001b. Geochemistry and petrogenesis of Iqna Sharaya volcanic rocks, Central Sinai, Egypt. *Egypt. J. Geol.*, (45/2), 921-940.
- Shapiro, L., and Brannock, W.W., 1962. Radio analysis of silicate, carbonate and phosphate rocks. *U.S. Geol. Surv. Bull.*, 1114 - A.
- Shatkov, G. A.; Shatkova, L. N., and Guschin, E. N., 1970. *Geochem. Int.*, 7, 1051-63.
- Shen, J., and Moore, P., 1982. Tiirnebohmite, RE<sub>2</sub>Al(OH)(SiO<sub>4</sub>)<sub>2</sub>: crystal structure and genealogy of RE(III)Si(IV)Ca(II)P(V) isomorphisms. *Amer. Mineral.*, 67, 1021-1028.
- Sherif, H. M.; Bousquet, R; Azab, M. S., and Gabr, M. M., 2007. Hamra Volcanics, Ras Naqab Area, Eastern Sinai, Egypt. *Geology, Geochemistry, Radioactivity And Chemistry Of Zircon. Proc. 7<sup>th</sup> Conf. Geol. Sinai for Development*
- Sherif, H. M., 1992. *Geology and radioactivity studies of Wadi El-Berra, south Sinai, Egypt. M. Sc. Thesis. Suez Canal Univ. Egypt.* 129 p.
- Shimron, A. E., 1980. Proterozoic island arc volcanism and sedimentation in Sinai, Precam. *Resh*, 12, 437- 458.
- Staatz, M. H., 1985. *Geology and description of the thorium and rare-earth veins in the Laughlin Peak Area, Colfax Country, New Mexico. Us Geol. Surv. Prof. Pap.*, E., 1-32.
- Stern, R. J., 1981. Petrogenesis and tectonic setting of Late Precambrian ensimatic volcanic rocks, Central Eastern Desert of Egypt. *Precam. Res.*, 16, 195-230.
- Stern, R. J., 1994. Arc assembly and continental

- collision in the Neoproterozoic East African orogen: implications for the consolidation of Gondwana land. *Ann. Review on Earth and Planetary Sci.*, 22, 319-351.
- Stern, R. J., and Hedge, C. E., 1985. Geochronologic and isotopic constraints on late Precambrian crustal evolution in the Eastern Desert of Egypt. *Am. J. Sci.*, 285, 97-127.
- Stern, R. J.; Kroener, A., and Rashwan, A. A., 1991. A Late Precambrian (~710 Ma) high volcanicity rift in the southern Eastern Desert of Egypt. *Geol. Rundschau*, 80, 155-170.
- Stern, R. J.; Sellers, G., and Gottfried, D., 1988. Bimodal dyke swarms in the North Eastern Desert of Egypt: significance for the origin of late Precambrian "A-type" granites in northern Afro-Arabia. In: *The Pan-African Belt of Northeast Africa and Adjacent Areas* (El Gaby, S., Greiling, R.O., Eds.). Vieweg, Weisbaden, 147-177.
- Stoeser, D. B., and Elliott, J. E., 1980. Post-orogenic peralkaline and calc-alkaline granites and associated mineralization of the Arabian Shield, Kingdom of Saudi Arabia. *King Abdul Aziz Univ., Jeddah, Bull. Inst., Applied Geology*, 4, 1-23.
- Sun, S. S., and Nesbitt, R. W., 1978. Geochemical regularities and genetic significance of Ophiolite basalts. *Geology*, 6, 689 - 693.
- Sylvester, P. J., 1989. Post-collisional alkaline granites. *J. Geol.*, 97, 261-280.
- Turner, S. P.; Foden, J. D., and Morrison, R. S., 1992. Derivation of A-type magma by fractionation of basaltic magma: An example from the Pathway Ridge, South Australia. *Lithos*, 28, 151-179.
- Walton, A.W.; William G., and Henry, Christopher, 1979. Release of uranium from volcanic glass in sedimentary sequences; an analysis of two systems.
- Whalen, J.B.; Currie, K.L., and Chappell, B.W., 1987. A-type granites: geochemical characteristics, discrimination and petrogenesis. *Contrib. Mineral. Petrol.*, 95, 407-419.
- Winchester, J. A., and Floyd, P. A., 1977. Geochemical discrimination of different magma series and their differentiation products using immobile elements. *Chemical Geol.*, 20, 325-343.
- Wood, D. A.; Joron, J. L., and Treuil, M., 1979. A re-appraisal of the use of trace elements to classify and discriminate between magma series erupted in different tectonic settings. *Earth Planet. Sci. Lett.*, 45, 326-336.
- Zielinski, R. A.; Lipman, P. W., and Millard, H. T., Jr., 1977. *Am. Mineral.*, 62, 426-37.
- Zielinski, R. A., 1978. Uranium abundances and distribution in associated glassy and crystalline rhyolites of the western United States: *Geol. Soci. Amer. Bull.*, 89, 409-414.
- Zielinsky, R. A., 1981. Experimental leaching of volcanic glass - Implications for evaluation of glassy volcanic rocks as source of uranium, *Amer. Assoc. Petroleum Geol. Studies in Geology*, 13, 1-11,
- Zielinski, R. A.; Lindsey, D. A., and Rosholt, J. N., 1980. The distribution and mobility of uranium in glassy and zeolitized tuff, Keg Mountain area, Utah, USA. *Chemical Geol.*, 29, 139-162.

## البركانيات الحمضية لأواخر عصر ما قبل الكمبري، جنوب سيناء، مصر: دراسة جيولوجية وإشعاعية

محمد صالح عزب

تضمن البحث دراسات حقلية، بتروجرافية، بتروكيميائية وإشعاعية للبركانيات الحمضية لمناطق وادي إقنا - جنوب سيناء، أم شوكي - جنوب شرق سيناء ثم بركانيات رأس النقب - شرق سيناء.

وقد خلص البحث إلى أن هذه البركانيات الحمضية لاحقة على بركانيات جبل الدخان، وأنها مشتقة في الأساس من صهارة ذات طبيعة فوق ألومينية إلى متوسطة الألومينية تكونت في بيئة داخل الألواح التكتونية. أوضح المسح الإشعاعي أن متوسط محتوى بركانيات رأس النقب من الثوريوم واليورانيوم ١٧، ١٥ جزء من المليون على الترتيب، كما أن متوسط محتوى بركانيات إقنا من الثوريوم واليورانيوم ١٧، ٩ جزء من المليون على الترتيب، أما بركانيات أم شوكي فمتوسط محتواها من الثوريوم واليورانيوم ١٧، ٩ جزء من المليون على الترتيب. وعلى هذا فمحتوى هذه البركانيات الإشعاعي يجعلها مصدرا هاما لعنصرى اليورانيوم والثوريوم، حيث أن متوسط محتواها من اليورانيوم يزيد عن ٨ جزء من المليون.

أمكن التعرف من خلال ميكروسكوب المسح الضوئي الإلكتروني على عدد من من المعادن مثل: الزركون، المونازيت، اليورانوثوريت والتروتوبهمايت.